UNITED STATES DEPARTMENT OF THE INTERIOR

GEOLOGICAL SURVEY

Gravity and aeromagnetic modelling of a large gabbroic body near the Border Ranges fault, southern Alaska.

By

Laurel E. Burns

OPEN FILE 82-460

This report was prepared in cooperation with the Alaska Division of Geologic and Geophysical Surveys.

This report is preliminary and has not been reviewed for conformity with U. S. Geological Survey editorial standards and stratigraphic nomenclature.

Any use of trade names is for descriptive purposes only and does not imply endorsement by the USGS.

CONTENTS

ILLUSTRATIONS

Table

Figure

Plate

ABSTRACT

A discontinuous, positive aeromagnetic and marine magnetic anomaly occurs on the northern side of the Border Ranges suture zone, a major tectonic boundary, in southern Alaska (Fischer, 1981). The magnetic anomaly occurs from near the southern Copper River basin to southwest of Kodiak Island, a distance of 1000 km, and suggests that the known outcrops of mafic and ultramafic rocks are much more continuous in extent than previously believed, and suggests a possible common source for the mafic and ultramafic bodies along this belt.

The largest outcrop in this mafic and ultramafic belt occurs between Tonsina and the Matanuska Glacier, approximately 160 km east of Anchorage. This study of the gabbro body was an attempt to increase the geologic knowledge of the mafic belt and the Border Ranges suture zone by integrating geophysical modeling techniques with geologic mapping. The gravity and aeromagnetic modeling suggests that a north-south cross-section of this gabbroic body is probably similar in shape to a trapezoid. The northern contact dips 20 to 40 degrees to the north, and the southern contact dips steeply, about 70 to 85 degrees, to the south. No preferred base for the gabbroic body was chosen from this modeling.

Unfortunately, no variation of silica content in the mafic body is evident from geologic mapping or geophysical modeling and no definitive statements about the structure of the Border Ranges suture zone can be made from the geophysical modeling.

The Border Ranges fault in this area appears to be a misnomer. The fault is mapped in this area as a steep to vertical fault (Plafker and others, 1977) and is defined as the major suture joining several different tectonic terranes (MacKevett and Plafker, 1974; Plafker and others, 1977). This steep fault is associated with very little penetrative deformation and occurs within tectonic melange zones which outcrop up to thirty km in width. The melange zones are characterized by cataclastic deformation, are structurally truncated by the steep Border Ranges fault, and appear to be the probable suture zone.

INTRODUCTION

Southern Alaska is presently thought to be a collection of allochthonous terranes (Jones and Silberling, 1979), fig. 1. A major suture zone joins the Chugach terrane on the south to several exotic northern blocks, including the Peninsular and Wrangellia terranes (MacKevett and Plafker, 1974; Jones and Silberling, 1979). The suture zone, of probable late Mesozoic or Early Tertiary age, includes major zones of melange, and can be traced from Kodiak Island to southeast Alaska, a distance of 2000 km (Plafker and others, 1979), fig. 2. Although traced for considerable lateral distance, the suture zone has not been mapped or described in detail in the literature. Clearly, understanding the nature of the regional tectonics requires a more detailed understanding of the nature of the suture zone. This paper represents an attempt to better describe the geometry and nature of the suture zone by combining semi-quantitative modeling of geophysical data with the known regional geologic mapping. The suture zone passes through the northwest Valdez and northeast Anchorage quadrangles, fig. 3. This area is the focus of this paper.

A steep to vertical fault within the suture zone has been termed the Border Ranges fault in this area and has been considered to be the principal thrust fault between the two terranes. This steep fault has very little penetrative deformation associated with it and differs markedly in its style of deformation from the melange zones (Burns, pers. obs., 1980; Pavlis, 1980; G. H. Pessel, oral commun., 1980), plate 1 (note: a simplified version is shown in fig. 3). Calling this particular fault the Border Ranges fault is probably a misnomer, and instead the melange zones really mark the major suture zone. Several other faults in this area, specifically the faults at the northern and southern boundaries of the melange zones, have been termed the Border Ranges fault (MacKevett and Plafker, 1974; Winkler and others, 1981). However, for simplicity, the Border Ranges fault referred to herein is the steep fault (Plafker and others, 1977) within the tectonic melange zones, fig. 3. The term "Border Ranges suture zone" will be used for the tectonic melanges. References to other investigations along the fault zone cause some confusion as to whether the tectonic feature discussed should be termed the Border Ranges fault or the Border Ranges suture zone. Such occurrences will be noted at the beginning of a paragraph with the probable tectonic feature in parentheses, following the usage in the reference.

A positive aeromagnetic and marine magnetic anomaly can be traced discontinuously, if not continuously, along the landward side of the Border Ranges fault (suture zone) from the southern Copper River basin to near Sutwik Island, southwest of Kodiak Island (Fischer, 1981), fig. 2. Ultramafic and mafic rocks are the probable source for this magnetic anomaly and are known to crop out in a discontinuous arcuate band on the northern side of the fault along its entire distance (Rose, 1966; Clark, 1972a; MacKevett and Plafker, 1974). The largest known mafic and ultramafic complex in this belt is the object of this study.

This gabbroic body and a two to twenty km wide tectonic melange are located between the recognized base of the Peninsular terrane (Talkeetna Formation) and the Chugach terrane. The mafic body subparallels the Border Ranges fault and crops out on its northern side, figs. 2 and 3. The body is composed dominantly of layered gabbro, but more silicic and more mafic rocks are included in the belt. This body extends from near Tonsina on the east to at least as far as the Matanuska Glacier, a distance of 120 km (Pessel and

Fig. 1: Cordilleran Suspect Terranes

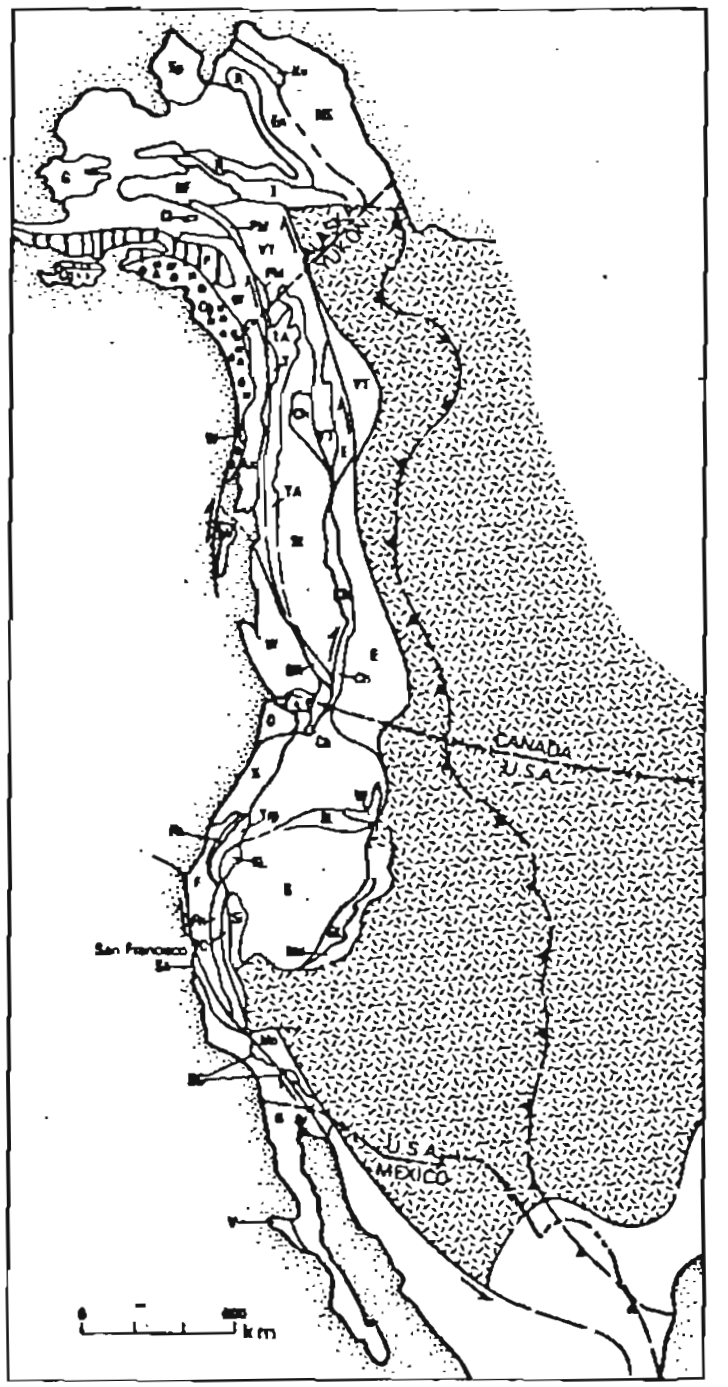

Fig. 1 Generalized map of Cordilleran Suspect Terranes. Dashed pattern, North American autochthonous cratonic basement. Barbed line, eastern limit of Cordilleran Mesozoic-Cenozoic deformation. Barbed arrows, direction of major strike-slip movement.

Peninsular terrane

Chugach terrane

modified from Coney et al. (1980)

Fig. 2: Generalized geologic map of southern Alaska, showing location of study area.*

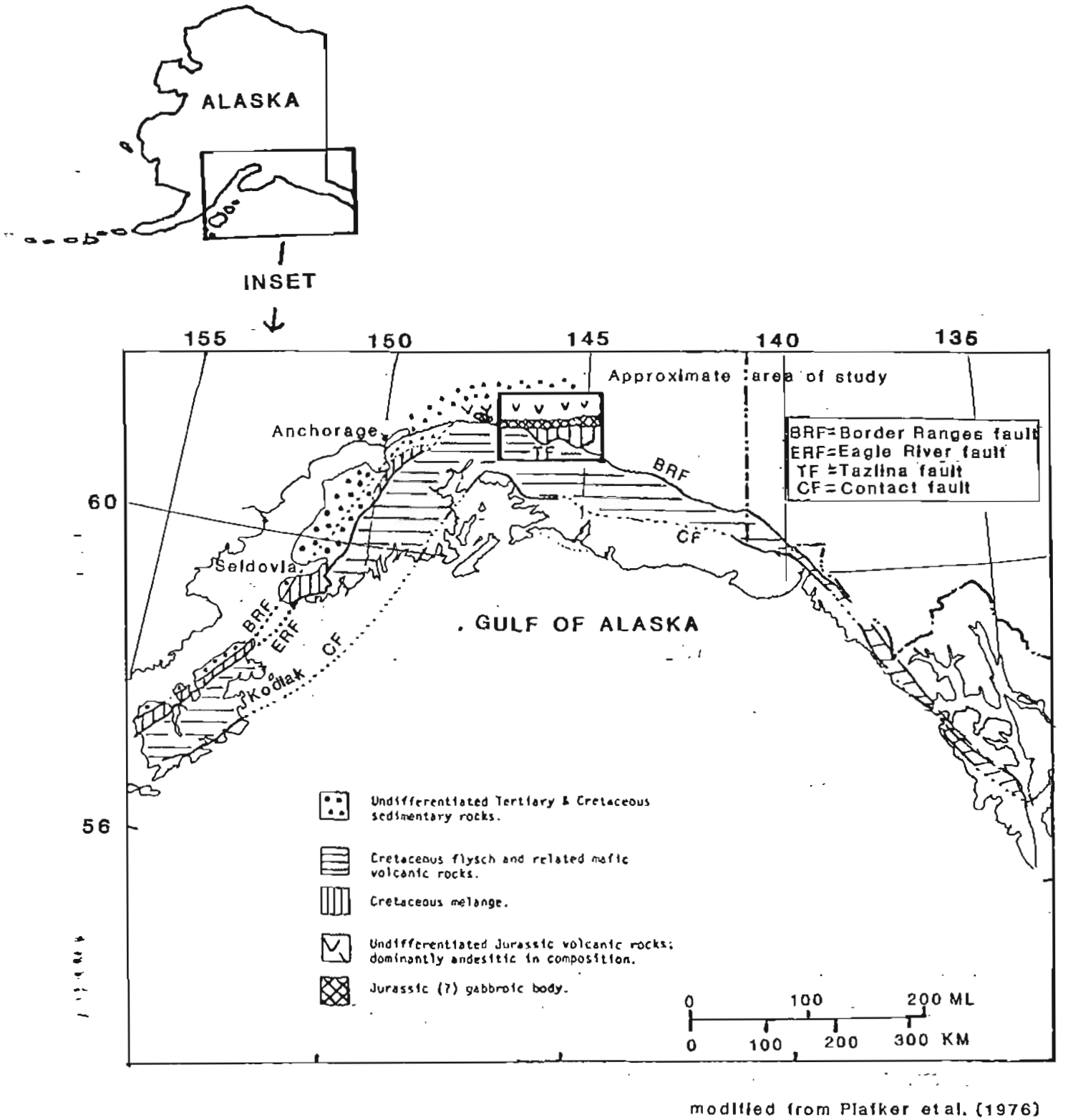

modified from Plafker et al. (1976)

* Location of faults approximate.

Figure 3: Generalized geologic map of the NE Anchorage and N Valdez quadrangles, Alaska

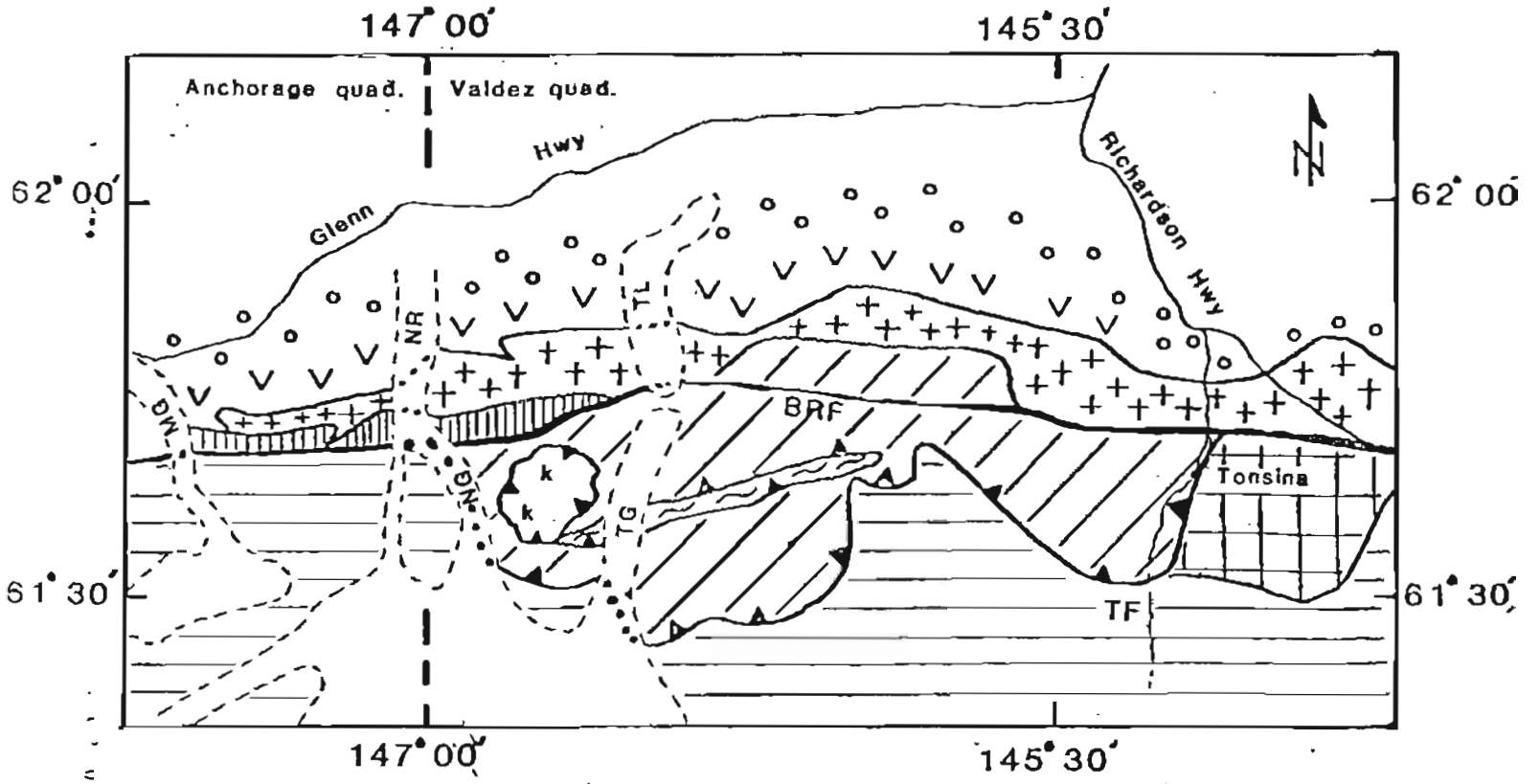

KEY

		fault
		thrust fault
	BRF	Border Ranges fault (Plafker et al., 1976)
	TF	Tazlina fault (Winkler et al., 1981)
	TG	Tazlina glacier
	TL	Tazlina lake
	NG	Nelchina glacier
	NR	Nelchina river
	MG	Matanuska glacier

ROCK UNITS

McHugh Complex; sedimentary melange of Triassic to Cretaceous age

North of the BRF

Cretaceous and younger sedimentary rocks, including Quaternary deposits.

Gabbroic melange of Cretaceous (?) or Tertiary (?) age.

Talkeetna Formation; Jurassic volcanic rocks.

Gabbroic body of Jurassic (?) age.

South of the BRF

Valdez Group; metasedimentary rocks of Cretaceous age.

Tonsina ultramafic complex of Jurassic (?) age.

Greenschist and transitional blueschist of Jurassic (?) age.

k Gabbro and amphibolite of Jurassic (?) age.

others, 1981; Winkler and others, 1981), and varies from two to ten km in width, covering about 1000 square km, fig. 3. Only reconnaissance geologic mapping and geophysical data exists west of the Matanuska Glacier in this area; thus the location of the western termination of the gabbroic body is not known.

Geologic mapping of the gabbro body is of reconnaissance nature at this time. Gravity and aeromagnetic modeling of the gabbro body was undertaken in order to add to the geologic knowledge of the area. Geophysical modeling was deemed appropriate due to the large gravity and magnetic anomalies caused by the gabbro body, the linear trend of the gabbro belt (allowing two-dimensional modeling), and the apparent absence of other dense or magnetic bodies influencing the anomalies. The following questions were addressed in this study.

1.) Is the Border Ranges fault steep at depth?
2.) Is the gabbro-volcanic contact north of the Border Ranges fault steep, as has been previously assumed (Grantz, 1961b, 1965; Pavlis, 1980)?
3.) Do the structure and composition of the gabbro change noticeably along its length?
4.) How deep does the gabbro extend?

PREVIOUS WORK

Geologic mapping in south-central Alaska is incomplete, and most of the existing mapping is reconnaissance in nature. The area between Kodiak Island and Anchorage, fig. 2, has the most extensive geologic mapping of the fault zone (Clark, 1972b; 1973; Connelly and Moore, 1979; Connelly, 1978). MacKevett and Plafker (1974) and Plafker and others (1977) have traced the Border Ranges fault in this area, but the central portion of the fault had not been mapped before 1979. Winkler and others (1981) mapped the gabbro body in the Valdez quadrangle in 1978 and 1979 at a scale of 1:250,000, and Pessel and others (1981) mapped the gabbro body in the Anchorage quadrangle at a scale of 1:63,360 in 1979 and 1980, fig. 3. Geologic mapping prior to 1979 particularly has not covered the gabbroic belt (Grantz, 1961a, 1961b, 1965; Andreason and others, 1964; MacKevett and Plafker, 1974; Plafker and others, 1977).

Geophysical data are similarly incomplete and composite. Case and MacKevett (1976) and Case and others (1979b) published aeromagnetic maps and geologic interpretations of small pieces of the Border Ranges fault in the McCarthy quadrangle to the east, and near Seldovia, southwest of Anchorage. The existing data consists of approximately 400 gravity stations established over the last 30 years (Andreason and others, 1964; Barnes, 1977; Case and others, 1979b), and two aeromagnetic surveys (Andreason and others, 1958; U. S. Geological Survey, 1979). No previous attempt has been made to quantitatively interpret this data.

PRESENT STUDY

This work represents the initial phases of an intensive study of the northeast Anchorage quadrangle. Regional mapping of the area in conjunction with G. H. Pessel and M. W. Henning of the Alaska Div. of Geological and Geophysical Surveys (ADGGS) was conducted over the 1979 and 1980 field seasons. During this period 105 gravity stations were established. Petrographic examination of approximately 50 thin sections was undertaken to confirm and extend field observations.

Geophysical modeling on data from the Valdez quadrangle was supported by the U. S. Geological Survey (USGS), and in part by National Science Foundation grant EAR80-01078.

DATA PREPARATIONS AND GEOPHYSICAL ASSUMPTIONS FOR MODELING:

The models presented in this paper should be viewed only as simplified possibilities. The computer techniques used for geophysical modeling assumed the gabbroic body was two dimensional. This assumption will not introduce much uncertainty, as the gabbro body is thin in outcrop relative to its width. The profiles were oriented at right angles to the geologic trend to minimize the error. A brief summary of the main simplifications and assumptions inherent in these geophysical models follows.

Gravity data:

Reduction of the gravity data was computed with a uniform density of 2.67 g/cm^3, see Appendix A. The simple Bouguer values are contoured at 5 mgal intervals, plate 2, and are assumed to be accurate to +/- 2 mgals.

Terrain corrections to a distance of 50 kilometers were made for the two modeled gravity profiles. A constant regional gravity field was assumed. The average density of the gabbro body, 2.92 g/cm^3, was sufficiently distinct from the densities of the adjacent rock belts, generally 2.72 g/cm^3, to allow modeling of the gravity profiles. However, the number of samples measured in a few of the units is not statistically valid, particularly given the variabilities in rock types (see Appendix A).

Magnetic data:

Three magnetic profiles were prepared from the 1979 aeromagnetic map, and two profiles were read from a combination of the 1979 and 1958 aeromagnetic maps. The estimated error in combining the two aeromagnetic maps is +/- 50 gammas. The combined aeromagnetic map is shown in plate 3. Small regional magnetic fields, decreasing from 3 to 12 gammas/ km to the south, were removed from the two magnetic profiles. The remanent magnetization was assumed to be in the same direction as the present earth's field (see Appendix B). The close correlation between the gravity and aeromagnetic models reinforces this assumption.

Simplifications:

Over-simplification of assumed constraints in magnetization and densities is probably the largest source of uncertainty, particularly in the magnetic models. The magnetization of the gabbro body varies considerably between neighboring outcrops. In most of the aeromagnetic models, the gabbro body is constructed of several large blocks with differing magnetizations, but large blocks of uniformly magnetized rock is an unlikely occurrence in this gabbro body.

For more detailed discussion, see Appendices A and B.

REGIONAL SETTING

The Border Ranges fault (suture zone) is a major tectonic boundary, over 2000 km. long, in south-central Alaska (Plafker and others, 1979). The fault trace is an arc from southwest of Kodiak Island (Fischer, 1981) to southeastern Alaska (Plafker and others, 1979), fig. 2. MacKevett and Plafker (1974) pointed out the significance of this fault as a late Mesozoic or Early Tertiary suture zone. The fault in the area of this survey is considered to be the boundary between two geologic terranes: Mesozoic plutonic and volcanic rocks (the Peninsular terrane) on the north, and a Mesozoic-early Tertiary accretionary complex composed of metavolcanic, sedimentary and metasedimentary rocks (the Chugach terrane) on the south, figs. 1 and 2.

GEOLOGY

Three major east-west trending belts of rock occur in the area of this report. These are, from south to north, (1) the McHugh Complex and Valdez Group of the Chugach terrane, (2) the gabbro belt, and (3) the Talkeetna Formation of the Peninsular terrane, fig 3. All three belts are intruded by Tertiary felsic intrusions, plate 1. These intrusives are not extensively deformed but appear to post-date major deformation of the melanges. Intermediate plutons of uncertain age and Tertiary andesite plugs intrude the northern terrane. The units are briefly described below.

1. Rock units south of the Border Ranges fault:

Two major rock units crop out south of the Border Ranges fault, fig. 3. The Valdez Group, a thick package of clastic marine sedimentary rocks, is presently thought to have been deposited in the Late Cretaceous (Tysdal and Plafker, 1978). The McHugh Complex, a sequence of volcanic and related sedimentary rocks, is considered to be a subduction melange (Clark, 1973; Winkler and others, 1981), and appears to be Triassic to mid-Cretaceous in age in this area (Winkler and others, 1981). A continuous belt, up to 4 km in width, of greenschists and transitional blueschists, occurs in the McHugh Complex, and crops out between the Nelchina Glacier and Klutina Lake, a distance of 40 km (Winkler and others, 1981).

The Tazlina thrust fault, a major tectonic feature, places the McHugh Complex over the Valdez Group (Winkler and others 1981), fig. 3. This thrust fault dips towards the Border Ranges fault and occurs discontinuously westward to the Anchorage area where it has been named the Eagle River thrust (Clark, 1972b, 1973; Winkler and others, 1981), fig. 2.

Another thrust fault, structurally overlying the Tazlina fault, places a small klippe of gabbro and amphibolite on top of the McHugh Complex, fig. 3. The klippe is located approximately 10 km. south of the Border Ranges fault in the western Valdez quadrangle. Magnetic modeling presented later in this

paper indicates that the klippe is approximately 300 meters thick. The source of the gabbro and amphibolite klippe is not known (Winkler and others, 1981).

2. Rock units north of the Border Ranges fault:

Two major belts of rock occur north of the Border Ranges fault, fig. 3. The southernmost belt, generally adjacent to the fault, is mainly composed of layered gabbros and minor amounts of ultramafic and intermediate plutonic rocks. Volcanic rocks of the Talkeetna Formation lie north of the gabbro belt. Both belts have similar structural styles, but the volcanic rocks are not as intensely deformed as the rocks in the gabbroic belt.

Plutons of intermediate composition intrude the gabbroic and volcanic rocks, plate 1, and probably range in composition from albite granite through trondjhemite and tonalite to diorite. The plutons are included in the crystalline melange zone and are quite deformed. Andesite porphyries of uncertain age intrude rocks north of the Border Ranges fault; these are too small to be included in the geologic map, or to affect geophysical models of the area, and are not considered further.

2a. Gabbroic belt:

The belt of gabbro trends approximately east-west, fig. 3. Large blocks of undeformed gabbro, one to two km in dimension, are separated by east-west trending shear zones of cataclastically deformed gabbro. Two sets of shear zones appear to be present. One set of shear zones, probably the oldest, dips gently to the north and is distinct from the second set of shear zones, which were produced by high-angle faults (Burns, pers. obs., 1980; G. H. Pessel, oral commun. 1981) affected most of the belt.

The outcrop belt is predominantly composed of layered two-pyroxene gabbros, hornblende gabbros, and leucogabbros. More silicic rocks (diorites and quartz diorites) and more mafic rocks, (peridotites, pyroxenites, and hornblendites) also occur. Dunites occur locally as pods or lenses in the mass of gabbro.

A tectonic melange, up to five km wide, fig. 3, crops out mainly on the southern boundary of the gabbro and consists dominantly of large chaotic blocks of relatively fresh gabbro in a matrix of serpentinite or sheared mylonitic gabbro. Exotic blocks, including several large blocks of the McHugh Complex, have also been mapped in this gabbroic melange zone, plate 1 (Winkler and others, 1981). The gabbroic melange is variable in thickness, and is covered or absent locally.

The gabbro appears to be intrusive into a package of high-grade metamorphic clastic sedimentary and metavolcanic rocks of unknown age. These rocks are known to crop out on the southern boundary of the gabbro, and in scattered placed throughout the gabbro, but occur in outcrops too small to be included in the geologic map at this scale.

2b. Talkeetna Formation:

The Talkeetna Formation, a package of marine and nonmarine volcanic

and volcanogenic sedimentary rocks, lies to the north of the gabbro body, fig. 3, and is dominantly composed of volcanic breccias, agglomerates, and water-laid tuffs of intermediate composition. The age of the volcanic rocks is well documented as Early Jurassic (Detterman and Hartsock, 1966; Detterman and Reed, 1980). Jones and Silberling (1979) state that the Talkeetna Formation forms the oldest exposed part of the Peninsular terrane.

Tracing beds is difficult, as the volcanic rocks are extensively deformed, though deformation is not as pervasive as in the gabbro belt (Burns, pers. obs., 1979; Winkler and others, 1981). The relationship of the gabbro to the volcanic rocks is not clear. The contact usually appears as a steep to vertical fault (Winkler and others, 1981; G. H. Pessel, oral commun., 1981; Burns, pers. obs., 1981).

3. Age of assembly and deformation:

The structural style of the McHugh Complex, dominantly south of the Border Ranges fault, is similar to the brittle deformation north of the Border Ranges fault, in the gabbro body and gabbroic melange are characterized by brittle shearing and extensive cataclasis, while the Border Ranges fault appears to be a clean break between rock units, which produced very little penetrative deformation (Burns, pers. obs., 1980; G. H. Pessel, oral commun., 1980; T. Pavlis, oral commun., 1980).

Limits for the age of deposition of the McHugh Complex (the subduction melange), and the age of two rock units incorporated into the gabbroic melange zone, north of the Border Ranges fault, provide time constraints for the age of accretion and associated deformation of these map units. Upper or Lower Jurassic cherts are included in the gabbroic melange zone, as is gabbro of probable Late Jurassic age (Winkler and others, 1981). Radiolarians from the McHugh Complex, generally south of the Border Ranges fault, place a lower age limit of mid-Cretaceous for the accretion of this subduction melange (Winkler and others, 1981). Both melanges are intruded by felsic intrusions that are relatively undeformed (Burns, pers. obs., 1980; Winkler and others, 1981), plate 1, and thus place an upper limit for the age of the major deformation. These intrusions in the McHugh Complex are believed to be Eocene in age (Winkler and others, 1981), and a probable age of Paleocene to Eocene (Grantz, 1960) has been suggested for felsites north of the Border Ranges fault.

Tertiary movement on the Border Ranges fault is indicated by the presence of a felsite pebble-bearing conglomerate which is locally caught up and deformed in the narrow fault zone (Pavlis, 1980; G. H. Pessel, oral commun., 1979; A. Grantz, oral commun., 1979), plate 1. Deformation of this conglomerate indicates post-Paleocene movement on the Border Ranges fault and, coupled with the differing structural styles in the melanges as compared to the Border Ranges fault, suggests that the steep Border Ranges fault is tectonically unrelated to the assemblage of these melange zones.

REGIONAL GRAVITY INTERPRETATION

Three gravity anomalies, all positive, are present on the simple Bouguer map, plate 2. The largest and most conspicuous gravity anomaly trends east-west and corresponds to the gabbro body. A southeastern extension of the anomaly is caused by mafic and ultramafic rocks, the Tonsina ultramafic complex, which were mapped by Winkler and others (1981) as a possible separate belt, and were not modeled in this study, fig. 3 and plate 2. The third and smallest gravity anomaly occurs between the Tazlina and Nelchina glaciers, to the south of the Border Ranges fault, plate 2. The contour lines bend to the south, away from the main gabbro body and correlate with the thrust klippe of gabbro and amphibolite on top of the McHugh Complex, fig. 3.

The 145 gravity stations established in 1979 and 1980 are concentrated between Tazlina Lake and the Matanuska glacier, see plate 2. Approximately 250 stations were established in the surrounding region during the past thirty years. About 150 of these stations are on the Richardson and Glenn Highways. Therefore, intensive gravity coverage is limited to the area between Tazlina Lake and the Matanuska glacier. Interpretation of the gravity anomaly is subject to uncertainty owing to the sparse number of gravity stations east of Tazlina Lake and in areas surrounding the gabbro body, such as the central Chugach Mountains.

GABBRO BODY

The conspicuous anomaly shown on the simple Bouguer anomaly map (SBA) is the 50 mgal high over the gabbro belt. The high trends east-west and is bordered on the north and south by simple Bouguer values of -60 to -70 mgals. Inspection of the SBA map indicates that the gravity anomaly associated with the gabbro body corresponds well, but not completely with the outcrop pattern of the body and that the SBA values appear to decrease to the east of Tazlina Lake.

Correlation of gravity anomaly with gabbro body:

West of Tazlina Lake, the gravity anomaly correlates extremely well with the geologic map. However, a discrepancy exists between the locations of the gabbro body and the gravity anomaly to the east of Tazlina Lake. The axis of the gravity anomaly appears to be centered on the southern edge of the gabbro body and extends southward into the metasedimentary rocks of the McHugh Complex. This discrepancy could conceivably be eliminated by terrain corrections, but inspection of the topographic map indicates that terrain corrections would probably increase the discrepancy. Because of rugged high topography of the Chugach Mountains on the south, gravity stations near the southern edge of the gabbro will have larger terrain corrections than stations established farther north. The larger terrain corrections would increase the positive anomalies over the McHugh Complex. The locational discrepancy could be a sampling problem as few gravity stations are established in this area. A likely possibility is that the gabbro body dips to the south in this region (see section

on magnetic interpretation and models)

East-west variation of simple Bouguer values:

East-west variation in the amplitude of the simple Bouguer values is evident from the map, plate 2. Gravity stations east of Tazlina Lake appear to have lower gravity values than stations to the west of Tazlina Lake. The apparent decrease in gravity values east of Tazlina Lake may be only a function of station spacing. SBA values for the 4 established gravity stations in the gabbro body east of Tazlina Lake range from -19 to -26 mgals. In comparison, the area west of Tazlina Lake has 25 gravity stations established on the gabbro body and range from about -33 to -10 mgals. Only 8 gravity stations in this area have SBA values above -19 mgals.

However, terrain corrections will probably increase rather than decrease the difference in gravity values between the east and west, because the topography is much gentler in the east. Terrain corrections on western stations are estimated to range from 4 to 12 mgals, as compared to 2 to 5 mgals in the east. (Values are estimated from established gravity stations which were terrain corrected by computer techniques and by hand.)

The lower gravity values east of Tazlina Lake are possibly due to the unknown thickness of sedimentary rocks and glacial deposits that covers most of the gabbro body in this area. A sediment thickness of 0.2 km would lower the SBA values due to the gabbro by approximately 2.5 mgals, assuming a density contrast of -0.3 g/cm^3. The decrease in SBA values may also be due to a variation of rock type, such as a more silicic phase of the gabbro to the east. The present data are inconclusive. See aeromagnetic interpretation for further discussion.

Compilation of a complete Bouguer anomaly map:

Compilation of a complete Bouguer map (CBA) would slightly alter the contour lines. A progressive decrease in terrain corrections would occur toward the north, because of increased distance from the Chugach Mountains. The resulting CBA map would increase the gravity anomaly near the southern portion of the gabbro body.

SMALL GRAVITY ANOMALY SOUTH OF THE BORDER RANGES FAULT:

A smaller positive gravity nose appears on the simple Bouguer map as a set of contour lines bending to the south, away from the Border Ranges fault, plate 2. The positive anomaly, approximately 10 mgals in amplitude, is present in the thrust sheet of the McHugh Complex between the Nelchina and Tazlina Glaciers. Because of few gravity stations, the amplitude and areal size of the anomaly can only be estimated. The anomaly apparently corresponds to the thrust klippe of gabbro and amphibolite that lies on top of the McHugh Complex, fig. 3.

AEROMAGNETIC INTERPRETATION

The aeromagnetic contour map, plate 3, can be divided into the following three major areas of distinctive magnetic character:

1. The area south of the Border Ranges fault, composed of essentially nonmagnetic metasedimentary and sedimentary rocks of the Valdez Group and McHugh Complex.
2. The gabbro belt having a positive magnetic anomaly of about 2000 gammas.
3. The area north of the gabbro belt, composed of weakly magnetized Talkeetna volcanic and clastic sedimentary rocks.

The few magnetic susceptibility measurements correspond with the same three major divisions. Measurements were made on various rock types within the area, but the mafic and ultramafic rocks had the only significant magnetic susceptibility. Case and others (1979b) have shown that the rocks of the Valdez Group and McHugh Complex are essentially nonmagnetic.

The Tonsina ultramafic complex and the thrust klippe of gabbro discussed in "regional gravity interpretation" are also apparent on the aeromagnetic map. In addition, the Twin Lakes positive anomaly, of approximately 500 gammas, is present in the northwestern part of the Valdez quadrangle. (Andreason and others, 1964). The source of this anomaly is not exposed, but may be an anomalously magnetized volcanic body within the Talkeetna Formation. Local variations in magnetic intensity in these volcanic rocks, particularly to the east of Tazlina Lake, are apparent in the aeromagnetic map and are probably due to magnetic units within the volcanic rocks, as discussed by Andreason and others (1964).

GABBRO BODY

The dominant feature on the aeromagnetic map is the large 2000 gamma high over the gabbro body. The conspicuous anomaly permits extrapolation of the gabbro body to the east, near Tonsina, beneath the sedimentary rocks of the Copper River basin. Inspection of the aeromagnetic map indicates several features. 1. The correspondence between the magnetic anomaly and the outcrop pattern of gabbro is extremely good. 2. The southern magnetic gradient of the gabbro body is generally steeper than the northern gradient, and a southern dip for the southern contact is implied in places. 3. An east-west variation in magnetic anomaly intensity and magnetic gradient is apparent; the intensity and gradient are lower in the eastern portion of the gabbro body. 4. A band of rocks having high magnetization and susceptibility crops out west of Tazlina Lake, in the western portion of the Valdez quadrangle, and is discussed in "the models".

Correlation of magnetic anomaly with gabbro body:

The aeromagnetic map, plate 3, appears to correspond well with the geologic map, plate 1. Unfortunately, the gabbro crops out discontinuously in the far eastern portion of this survey and the faults shown in this area on the geologic map have been partly inferred from the aeromagnetic map (Winkler and others, 1981). The anomaly correlates well where the gabbro outcrops are continuous, i. e. west of Tazlina Lake.

The aeromagnetic anomaly does not extend southward over the McHugh Complex east of Tazlina Lake, as the SBA gravity anomaly appears to do. The location of the contact in this area was inferred from the geologic mapping, instead of from the aeromagnetic anomaly (Winkler and others, 1981). The difference in distance dependence of gravitational and magnetic fields resolves the apparent conflict between aeromagnetic and gravity data. A gabbroic body at considerable depth could cause a gravity anomaly without causing a measurable magnetic anomaly. The magnetic gradient and two modeled aeromagnetic profiles , figs. 19-23, in this area probably imply a southward dip of the gabbro body (see section on the models).

General nature of contacts:

The magnetic gradient on the southern contact of the gabbro is generally steeper than the gradient on the north, implying a steeper dip for the southern boundary of the gabbro. Both the magnetic and gravity models agree with this interpretation (see "models").

East-west variations in the aeromagnetic anomaly:

The magnetic intensity, relief, and gradients on the northern and southern edges of the gabbro appear to vary on the aeromagnetic map from east to west. The magnetic intensity shown on the aeromagnetic map appears to decrease to the east of Tazlina Lake. The average magnetic intensity in the eastern section of the gabbro body is approximately 1000 gammas lower than the magnetic intensity to the west, approximately 2000 gammas. The magnetic relief in the eastern portion of the aeromagnetic map is thus approximately 1000 gammas lower than the relief in the western portion, as the surrounding regions appear to have the same magnetic intensity in the east and west.

The change in the magnetic intensity to the east could be caused by several factors, similar to the factors controlling the possible decrease in gravity values on the SBA map. The decrease in magnetic intensity may be a factor of increasing depth of sedimentary cover over the gabbro body, or a change in the magnetic properties of the rocks. The magnetism of these rocks presumably correlates inversely with silica content. A general increase in a silicic phase of the gabbro to the east would explain the eastward decrease of the anomaly. No major magnetic susceptibility trends within the gabbro body were noticeable from measurements made in this survey. However, there were too few susceptibility measurements made to define a trend, given the scatter of susceptibilities for samples from an individual station.

A decrease in magnetic intensity would occur with smaller outcrops of gabbroic rocks. The positive magnetic anomalies east of Tazlina Lake correspond well with the gabbro outcrops. This correlation implies that the depth and areal extent of the sedimentary rocks east of Tazlina Lake probably

Table 1

Approximate Aeromagnetic Gradients of Gabbroic body

Profile	Gradient (gammas/km)	
	Southern Contact	Northern Contact
West of Tazlina Lake	190-250	160-250
East of Tazlina Lake	90-190	60
Near Tonsina	90-125	60

are the main factors controlling the level of magnetic intensity.

The steepness of magnetic gradients on the northern and southern boundaries of the gabbro body also decreases to the east, see table 1. Shallower dips for the boundaries of the gabbro body would decrease the magnetic gradient. However, because the intensity of the magnetic anomaly varies also, sedimentary deposits or a change in the magnetic properties of the gabbro body are more likely sources for the change in the magnetic gradient (see models).

THE MODELS

GABBRO BODY

Modeling of gravity and aeromagnetic profiles yielded information about the attitude of the northern and southern contacts of the gabbro body, and the variation of rock types within the body. Five aeromagnetic and two gravity profiles, plates 2 and 3, were modeled using standard techniques (see Appendices A and B). The profiles were oriented north-south, perpendicular to the trend of the gabbro belt, and lie approximately between 145° 30' and 147° 00' W. long (see plates 2 and 3). Two models, with gabbro depths of approximately three to eight km., were computed for each individual profile.

The computed models resemble a trapezoid. The northern contact dips 20 to 40 degrees to the north and the southern contact appears to be steeper, with dips generally 70 to 85 degrees to the south. No significant east-west variation in dip of the bordering contacts was noticed in the models. Table 2 summarizes the contact angles for each model. A flat bottom of the gabbro was modeled in the profiles, but other irregular bases for the gabbro mass could fit the data equally well. Gravitational and aeromagnetic effects correlate inversely with depth, allowing wide variation in the structure and physical properties of the lower parts of modeled bodies.

Determination of an optimal depth to the base of the gabbro body was not possible in this study, because of insufficient data and the assumptions made for the simplified models. The number of magnetic susceptibility measurements is not large enough to accurately depict the variation of physical properties of the gabbro body on the surface, and the physical properties of the gabbro at depth can only be assumed. Slightly higher magnetizations and higher density contrasts are generally required in the shallow models, as compared to the deeper models, but all densities and magnetizations used in both models are geologically reasonable.

Comparison between gravity and aeromagnetic models:

The gravity and aeromagnetic models appear to compare favorably. One gravity and one magnetic profile are located in the same location, and models for this profile are shown in figs. 4 and 5. The gravity models are wider than the aeromagnetic models. The contacts of the gabbro body probably occur between the gravity model contacts and the aeromagnetic model contacts. Unfortunately, the geologic mapping can not determine the exact location of the contacts in this area because of sedimentary strata and the presence of Tazlina Lake. The difference in dip of the contacts in the gravity and aeromagnetic models is generally within the uncertainty of the models, approximately 10 degrees.

Northern contact:

Previous reconnaissance geologic mapping assumed that the gabbro-volcanic contact was steep to vertical (Grantz, 1961b, 1965; Pavlis, 1980). This study indicates a low to moderate dip to the north, from 20 to 40 degrees, for this contact, table 2, but a vertical fault, as shown in fig. 27, could still be

TABLE 2.

GEOPHYSICAL MODELS

SUMMARY OF CONTACT ANGLES

GRAVITY/ MAGNETIC MODEL	SHALLOW MODELS		DEEP MODELS	
	northern contact	southern contact	northern contact	southern contact
GA1			20 deg. N	75 deg. N
GA2	15 deg. N	40 deg. S		
GA3			20 deg. N	60 deg. S
GB1	15 deg. N	65 deg. S		
GB2			25 deg. N	80 deg. S
A1	25 deg. N	70 deg. S		
A2	25 deg. N	70 deg. S		
A3			40 deg. N	85 deg. N
B1	20 deg. N	40 deg. S		
B2			35 deg. N	80 deg. S
C1	20 deg. N	55 deg. S		
C2	25 deg. N	45 deg. S		
C3			45 deg. N	80 deg. S
D1	15 deg. N	50 deg S		
D2			25 deg. N	75 deg. S
E1	25 deg. N	45 deg. S		
E2	15 deg. N	60 deg. S		
E3			40 deg. N	75 deg. S

present and would probably not show up in the geophysical models. Deeper models with approximately 6 to 8 km of gabbro indicate a northern contact dipping 35 to 40 degrees to the north. Shallower models with approximately three km of gabbro need a northern contact dipping 20 to 25 degrees to the north.

Significant changes in the residual gravity and aeromagnetic data would have be necessary to steepen the northern contact more than 10 degrees, and none of the estimated changes would change the nature of this contact from shallow to steep. A decrease of 20 mgals in complete Bouguer values in the southern portion of the gravity profiles would change the assumed regional gravity field from constant (assumed in this study) to approximately 0.4 mgal/km decreasing to the south, and would require a steeper dip for this contact, approximately 10 degrees. The CBA values are probably accurate to +/- 10 mgals, thus an assumed regional field decreasing this rapidly to the south is unlikely.

A lower density contrast between the volcanic rocks and the gabbro body would increase the dip of this contact. The density contrasts generally assumed in the gravity models were 0.20 and 0.25 g/cm^3. Only 14 density determinations on the volcanic rocks were made in this study. The densities range from 2.61 to 2.90 g/cm^3, with the average values being 2.72 g/cm^3. This value is normal for intermediate volcanic rocks and was used in the gravity models. Andreason and others (1984) determined densities on 38 "Jurassic and older volcanic rocks" from the Copper River basin. The majority of the rocks were from the Talkeetna Formation (D. Barnes, 1981, oral commun.). Their study showed an average density of 2.64 g/cm^3. The density contrast may be greater than that used in the gravity models, and would imply an even shallower dip for the northern contact.

The volcanic rocks of the Talkeetna Formation were not included in the models as being magnetic, and their omission from the magnetic models seems justified. The 11 magnetic susceptibility measurements on these volcanic rocks imply a very low magnetic susceptibility for this formation, approximately 0.001 emu/cm^3. However, magnetization of these volcanic rocks is variable (Andreason and others, 1984). Local basalt flows may contribute to magnetic anomalies and are the probable cause of the slightly shallower angle for profile D-D'.

Southern contact:

Most gravity and aeromagnetic models suggest a southern dip for the southern contact of the gabbro body, table 2. Only two models, figs. 6 and 13, required a northward dipping contact of approximately 85 degrees. Uncertainties in the geologic maps, and the assumption of simplified bodies, probably introduces an error of +/- 15 degrees for the angle of this contact.

This steep southern angle does not necessarily imply a solid mass of gabbro that dips steeply to the south. The gabbro body could be composed of several thrust slices dipping to the north, fig. 28. No distinctions between a northward dipping or southward dipping structure of the gabbroic melange can be made on the basis of these geophysical models. Geologically conceivable models, with the gabbroic melange zone dipping either to the south or north, can be made to fit the geophysical data. A northward dipping gabbroic melange is shown on fig. 6, the gravity traverse in the Nelchina valley.

The gabbroic melange zone is generally neglected in the gravity and magnetic models. This omission only affects one gravity profile, as the Tazlina Lake

gravity profile does not cross much, if any, gabbroic melange, fig. 9 and 10. The gravity profile in the Nelchina valley crosses approximately 2.5 km of gabbroic melange, figs. 6-8. Unfortunately, density determination of this melange is difficult. Gravity models were computed using melange-gabbro body density contrasts of 0.0,0.1, and 0.2 g/cm^3, with the gabbro body being the densest body. All models could be made to fit the gravity data.

Omitting the gabbroic melange zone from magnetic profiles A and B, figs. 11-15, appears to be justified as the magnetization in the melange does not appear to be strong. Magnetic susceptibility measurements on samples from the melange showed slight values, approximately 0.0005 emu/cm^3, see Appendix B. The aeromagnetic map also does not imply a large magnetization for the gabbroic melange zone. The presence of a slightly magnetized gabbroic melange dipping to the north, into the gabbro body, can easily be masked by the magnetic signature of the gabbro.

Magnetic profile E, figs. 21-23, crosses the block of McHugh Complex that crops out between the gabbro body and the Border Ranges fault east of Tazlina Lake. No gabbroic melange was mapped in this area. The SBA gravity map indicates a discrepancy between the gravity anomaly and the gabbro outcrops in this area. A southward dip of the gabbro body is indicated by the magnetic model. The model correlates well with interpretation of the gravity and aeromagnetic anomaly in this area. However, the greater thickness of sedimentary rocks in this area makes the dip of this contact uncertain.

Border Ranges fault:

The dip of the Border Ranges fault could not be accurately determined in this study. Geologic mapping and the geophysical models imply that the Border Ranges fault is steep to at least a depth of 3 km. The relatively unaltered gabbro body, as opposed to the gabbroic melange, crops out near or adjacent to the Border Ranges fault in profiles GB (gravity) and C (aeromagnetic), and is shown in figs. 4, 5, 9, 10, and 16-18. The gravity profile indicates a southern dip for the Border Ranges fault, but the exact location of the fault in this area is not known due to glacial deposits, and control for the regional gravity field is poor in this area. No gravity stations exist immediately south of the gabbro body. The aeromagnetic models do not require that the gabbro body extend south of the Border Ranges fault.

The other profiles suggest that the relatively unaltered gabbro body generally dips toward the Border Ranges fault and probably approaches the fault at depths of at least three km, fig. 6-27. Interpretation of gravitational and aeromagnetic effects from bodies at depth is ambiguous and many models will produce computed profiles similar to the observed profiles. Thus, no definitive statement concerning the dip of the Border Ranges fault can be made from these geophysical models.

Alternate remanent magnetic field directions:

Several magnetic models were computed with varying directions of the gabbro's magnetization, and are shown in figs. 24-26. The dip of the northern contact increases by approximately 5 degrees and the southern contact stays

approximately the same when the assumed declination is increased from 28 degrees to 60 degrees. Decreasing the assumed declination to 15 degrees increases the dip of the southern contact to nearly vertical, while not altering the northern contact.

Magnetic zones:

The gabbro body was generally modeled by using several different magnetic zones within one magnetic profile. Large edge effects generally occur when only one magnetization for the gabbro body is modeled, fig. 11. The edge effects are produced by the contrast in magnetization of the gabbro and surrounding rocks, and the angles of the gabbro's contacts. Zones of differing magnetic intensity were added to the models in order that the modeled profiles fit the observed profiles. The magnetic zones trend east-west across the gabbro body and imply continuity of magnetization laterally within the gabbro body. The zones should be viewed only as possible models, and detailed mapping, petrography, and magnetic susceptibility measurements are necessary to determine whether these simple zones are actually present. The northward dip of these zones can generally be varied about 10 degrees, but could not be made to dip parallel to the northern contact and fit the aeromagnetic profiles unless magnetically complicated bodies were used. Thus no definitive configuration for the magnetic zones can be determined from the models.

One distinct magnetic zone does exist, as judged from susceptibility measurements and inspection of the aeromagnetic map, plate 3. This magnetic zone occurs in the western part of the Valdez quadrangle and appears to vanish just east of Tazlina Lake. Geologic mapping (plate 1), magnetic susceptibility, and the magnetic models support this observation. This zone corresponds with a large shear zone, which contains peridotites, and tectonic inclusions of serpentinites (Winkler and others, 1981). The shear zone, up to about 0.4 km. wide (J. E. Case, oral commun., 1981), crops out in the middle of the exposed gabbro body, and can be traced to the west across the Nelchina River valley, to the vicinity of the South Fork of the Matanuska River. In this area, the shear zone is exposed at the northern contact of the gabbro and separates the gabbro from the volcanic rocks (Pessel and others, 1981).

Ultramafic rocks:

The Nelchina valley traverse, figs. 6-8, shows a complex gravity profile composed of a broad 30 mgal high with a narrow superimposed 20 mgal peak. This peak correlates with a band of ultramafic rocks, approximately 0.7 km wide, located within the gabbroic body. These ultramafic rocks are dominantly peridotites, as judged from preliminary thin section examination (G. H. Pessel, oral commun., 1981). This narrow peak is not observed on the next traverse to the east, figs. 9 and 10, and gravity stations are too sparsely located between the Tazlina and Nelchina traverses to detect a small ultramafic body. The lack of geophysical data combined with the lack of detailed geologic mapping precludes delineation of an ultramafic body in the area.

A density value of approximately 3.2 g/cm^3 is implied for the ultramafic rocks, as a density contrast of 0.25 g/cm^3, between the gabbro and the ultramafics, produced the best fit gravity profiles, and about 2.92 g/cm^3.

East-west variations:

The angles of the contacts bordering the gabbro body do not seem to change significantly along the section of gabbro modeled, table 2. Profile E crosses the McHugh Complex north of the Border Ranges fault instead of the gabbroic melange zone, like most of the other profiles. No major differences in the southern contact exists between model E and the other models. Profile D has a shallower northern contact than the other profiles, which is probably produced by interference by some local anomaly in the Talkeetna Formation, as judged by inspection of the aeromagnetic maps.

The main east-west variations implied from the geophysical modeling concern the magnetization. The magnetization appears to increase slightly from east to west. The highly magnetic shear zone west of Tazlina Lake is probably the major cause of this variation. An additional source for the decrease in measured magnetic intensity, and hence lower magnetizations used in the models, is the increased thickness in sedimentary cover in the eastern portion of the gabbroic body. The positive magnetic anomalies correspond extremely well with individual outcrops of gabbro.

SMALL ANOMALY SOUTH OF THE BORDER RANGES FAULT

A small positive bullseye-shaped anomaly, about 100 gammas in amplitude, exists south of the Border Ranges fault. The high is coincident with the thrust klippe of gabbro sitting on top of the McHugh Complex. Profiles A and B, figs. 11-15, cross this southern anomaly, and imply that it is about 300 meters thick.

TWIN LAKES ANOMALY

The Twin Lakes positive anomaly, about 400 gammas in amplitude, in the northwestern part of the Valdez quadrangle occurs over the sedimentary strata of the Talkeetna Formation. Andreason and others (1964) interpreted the anomaly as as anticline bringing magnetic volcanic rocks near the surface. Model F1, fig. 29, implies that the magnetization of the anomalous body must be much higher than the magnetization of the volcanic rocks measured in this survey. Best fits were produced with models using a magnetization of 0.003 emu. This value is suggestive of basalt or an igneous intrusion. Basalt flows are common in the Talkeetna Formation and are the probable cause for the anomaly. A magnetic Tertiary intrusion could possibly cause the anomaly. However, no known Tertiary intrusions are significantly magnetic in this area. The gabbro body is apparently the only known plutonic rock with significant magnetization, and cannot be completely dismissed as the possible source, either as a fault sliver, or an intrusion into the volcanic rocks beneath the sedimentary sequence.

Figure 4: Comparison of gravity and magnetic models for shallow gabbro body--
Tazlina Lake profiles

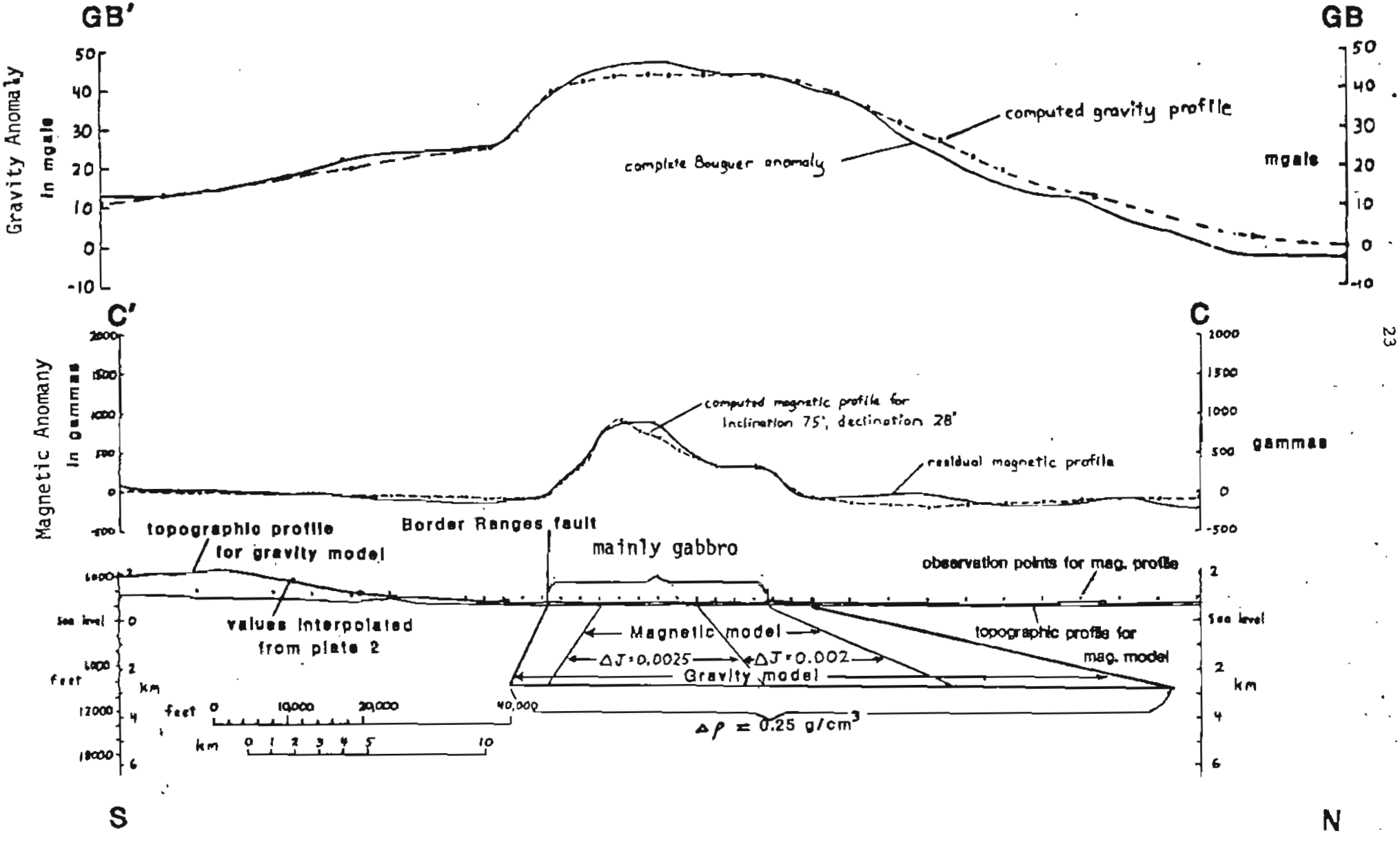

Figure 5: Comparison of gravity and magnetic models for deep gabbro body--
Tazlina Lake profiles

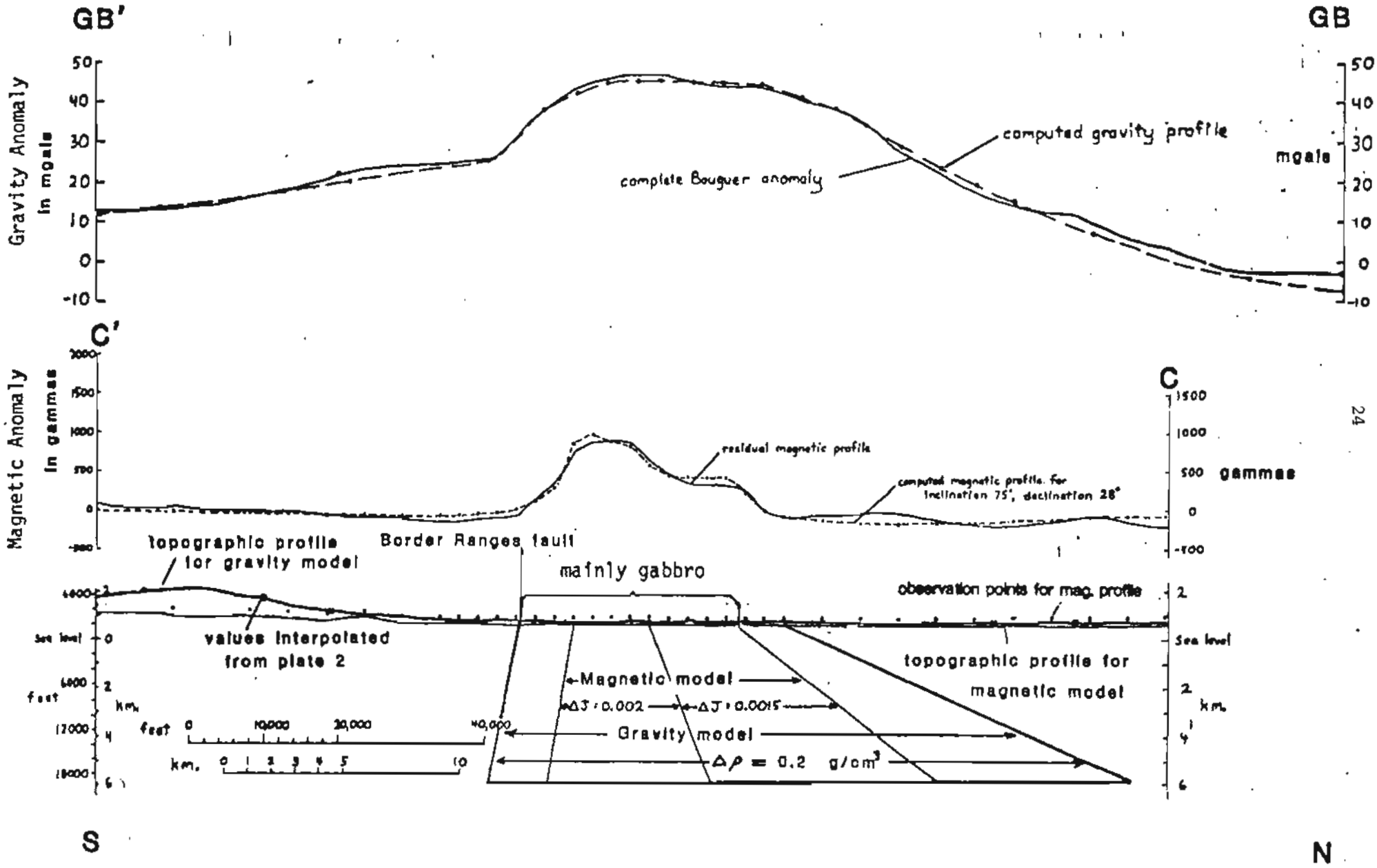

Figure 6: Gravity profile through the Nelchina Valley
Model GA1

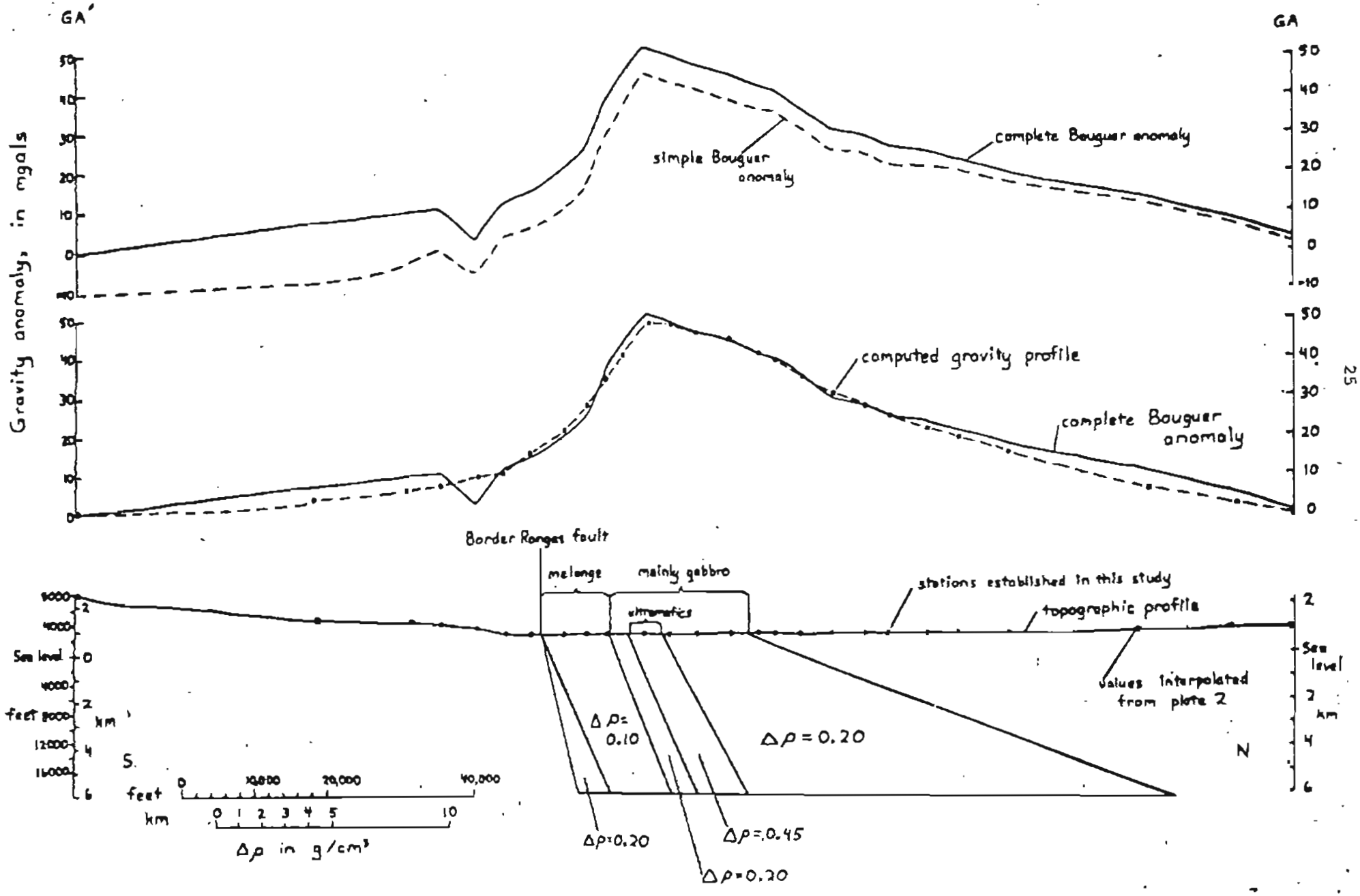

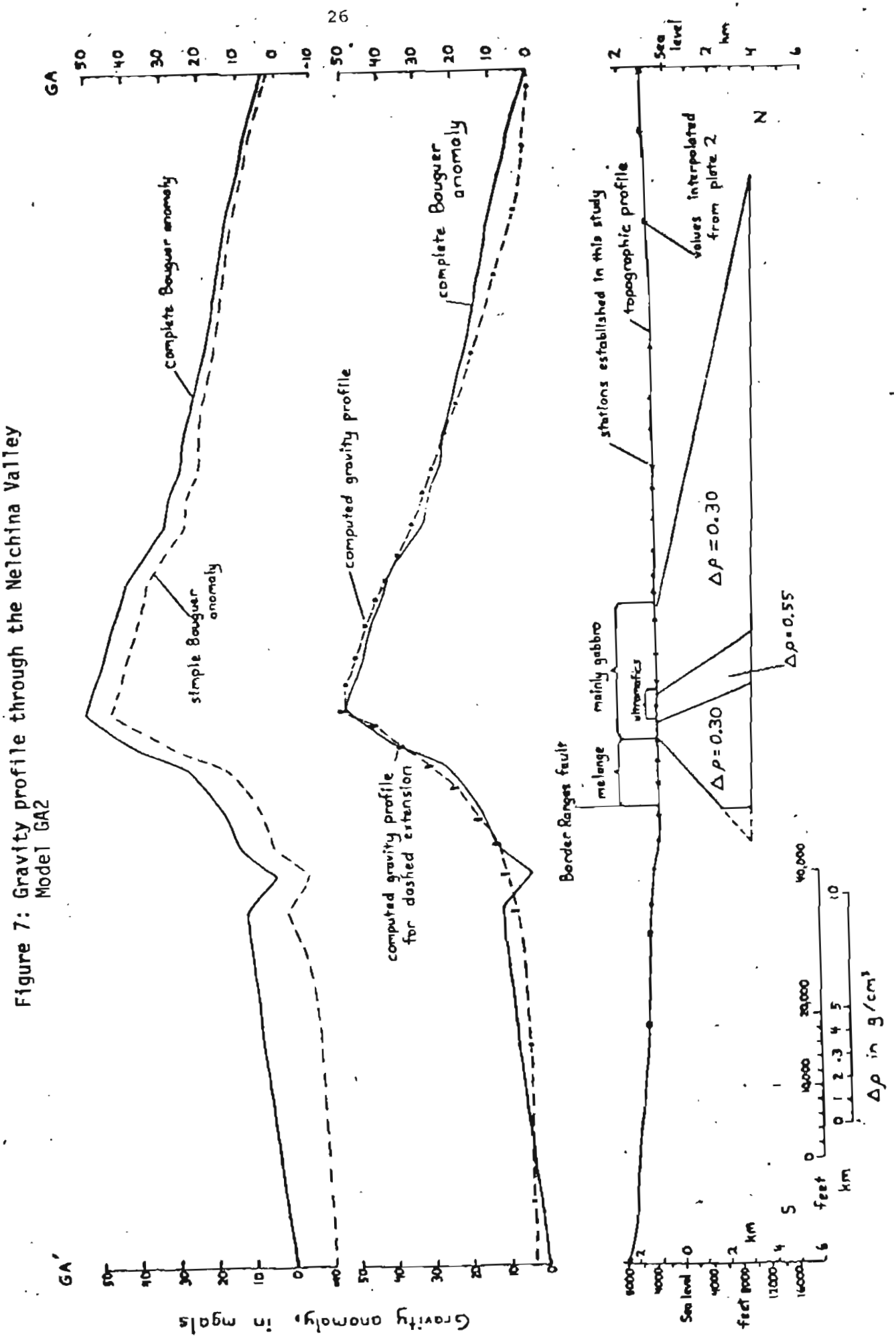

Figure 7: Gravity profile through the Nelchina Valley
Model GA2

Figure 8: Gravity profile through the Nelchina Valley
Model GA3

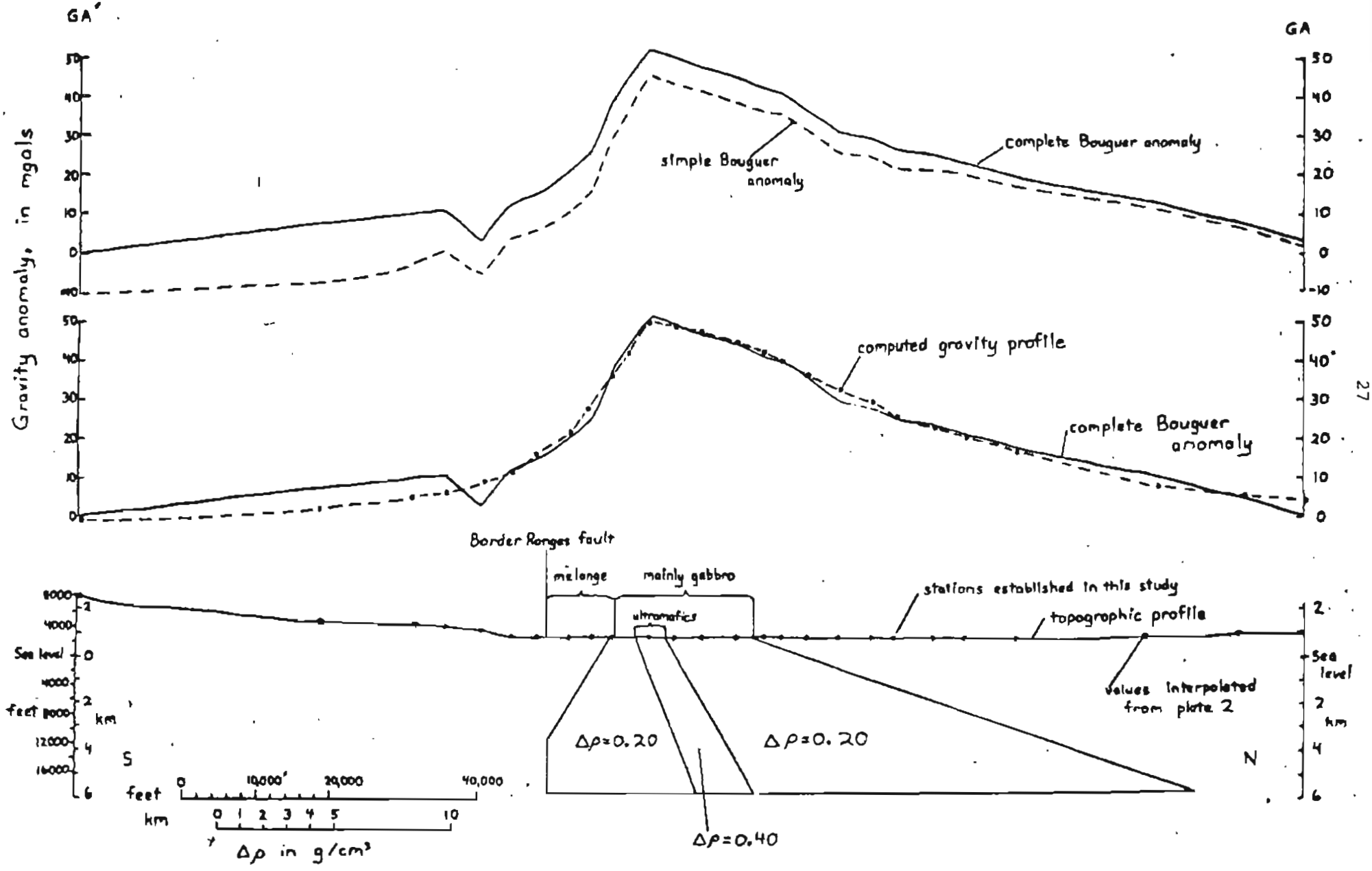

Figure 9: Gravity profile near Tazlina Lake
Model GB1

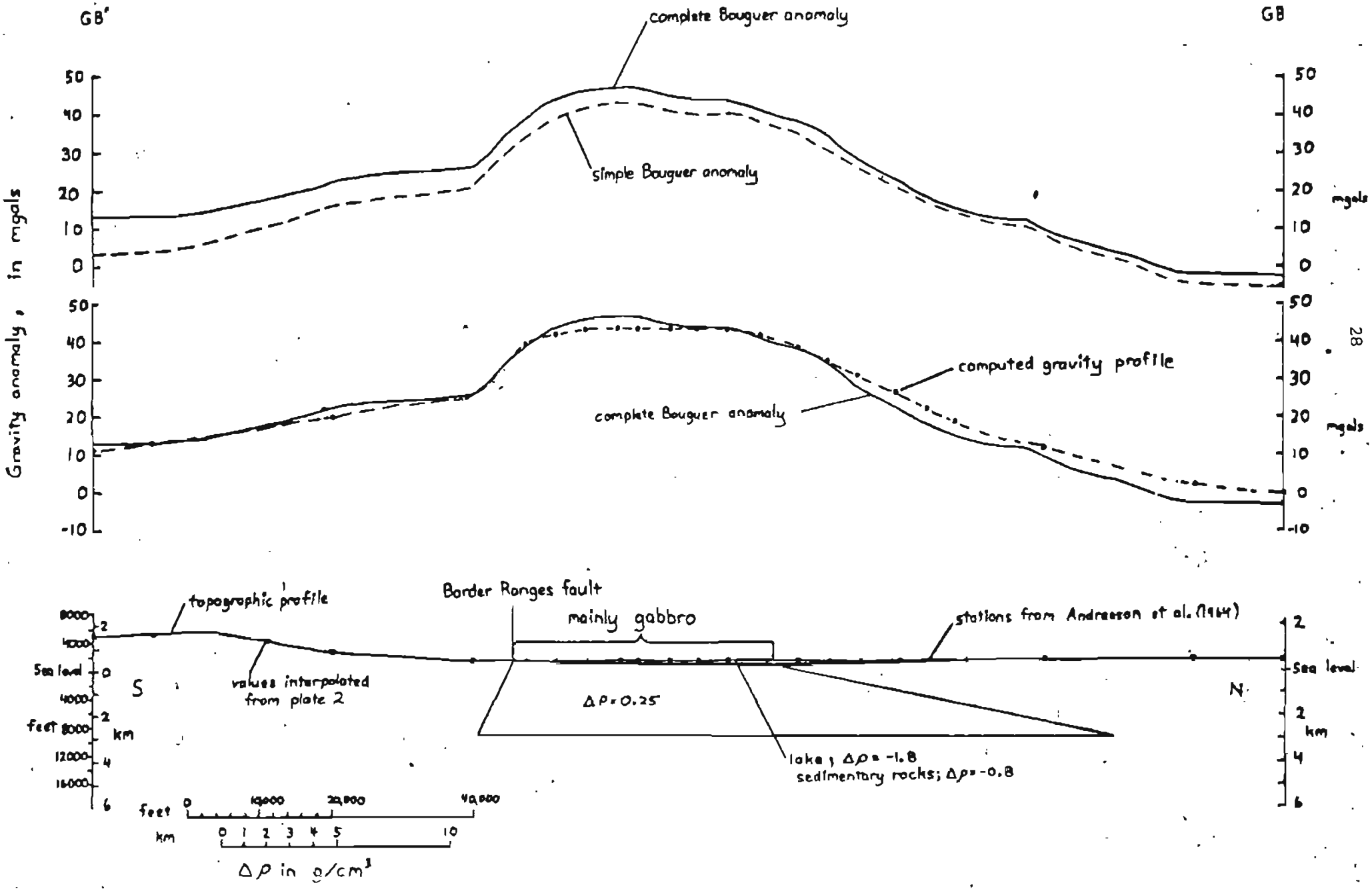

Figure 10: Gravity profile near Tazlina Lake
Model GB2

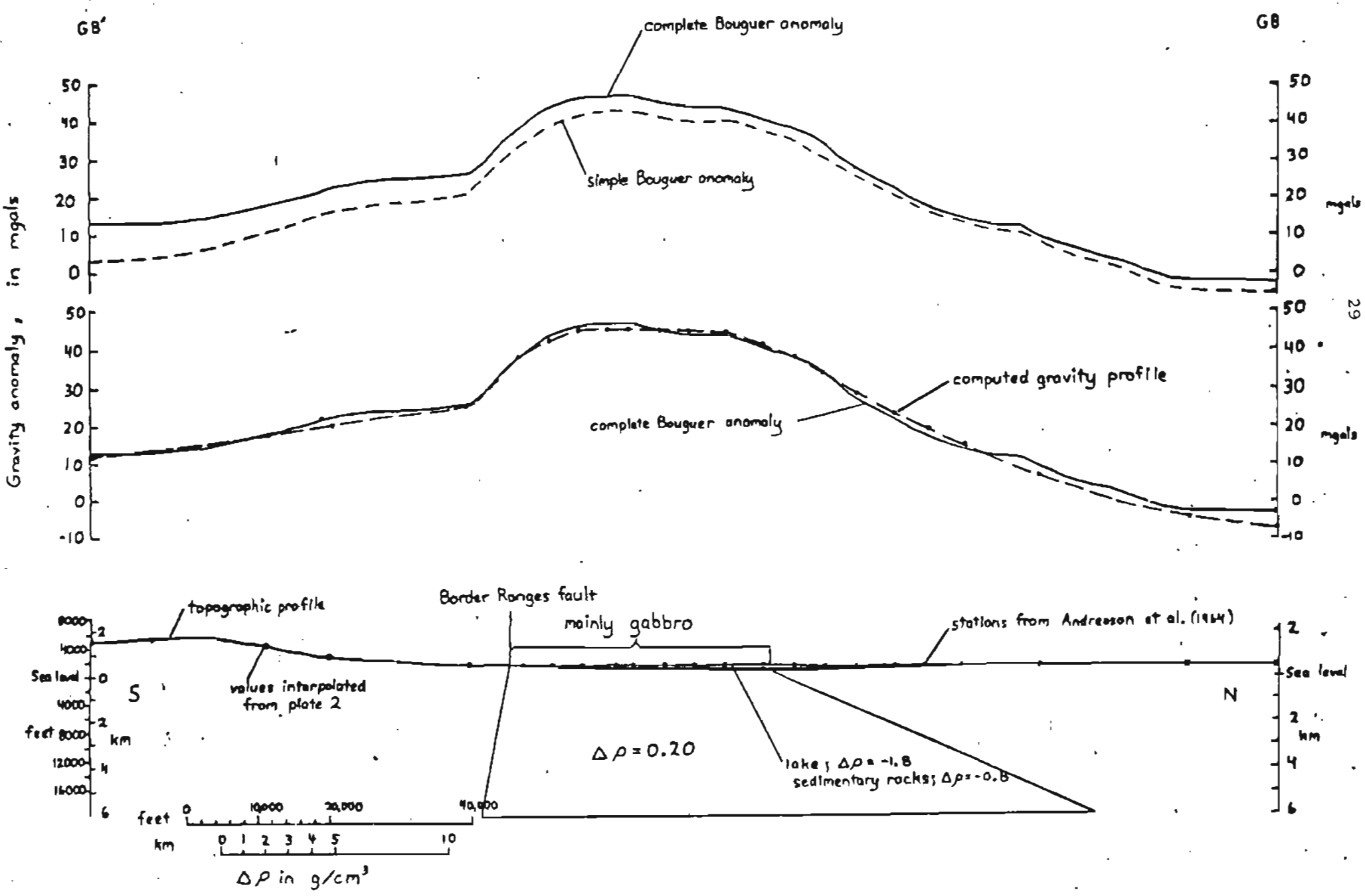

Figure 11: Aeromagnetic profile west of Tazlina Lake
Model A1

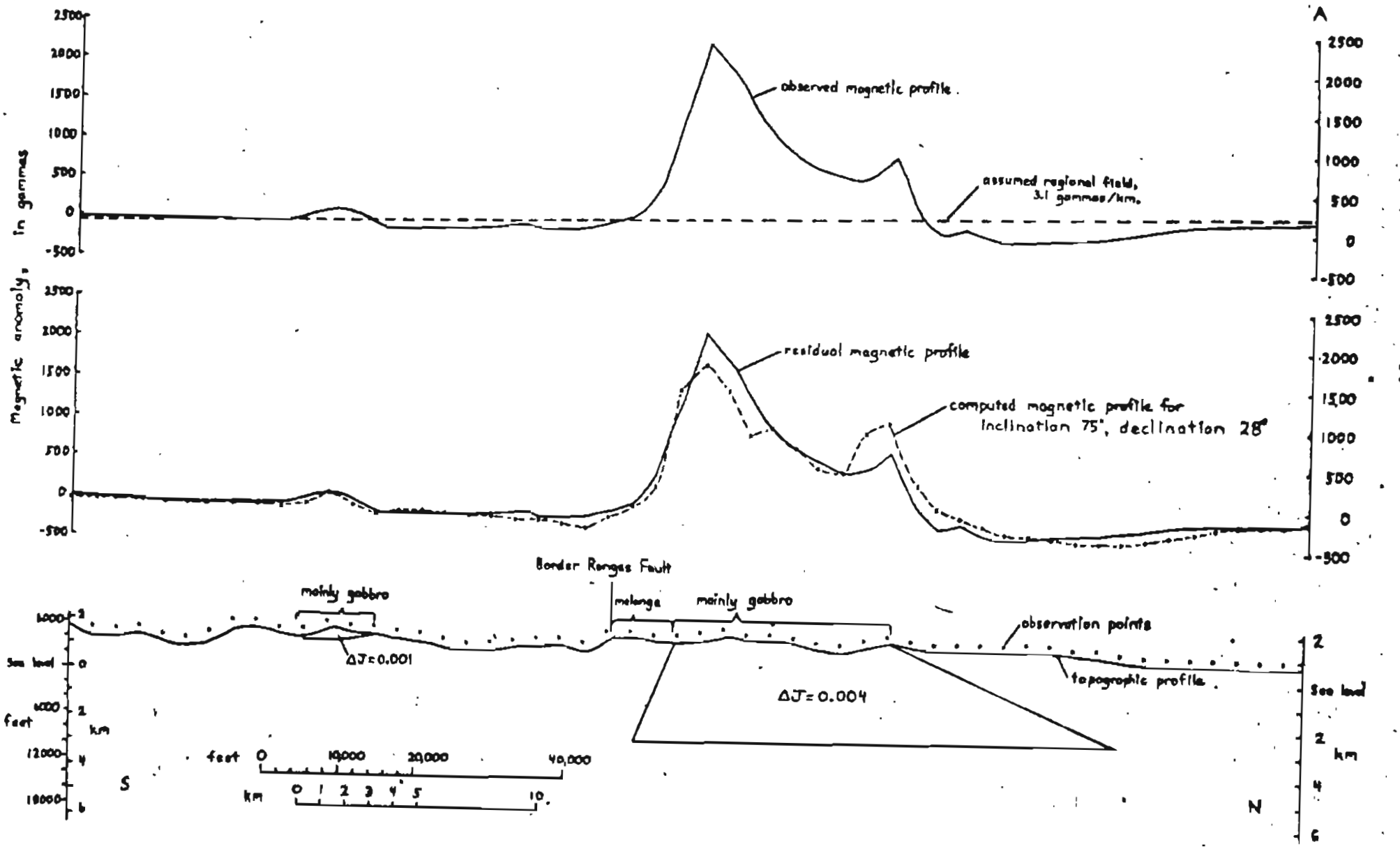

Figure 12: Aeromagnetic profile west of Tazlina Lake
Model A2

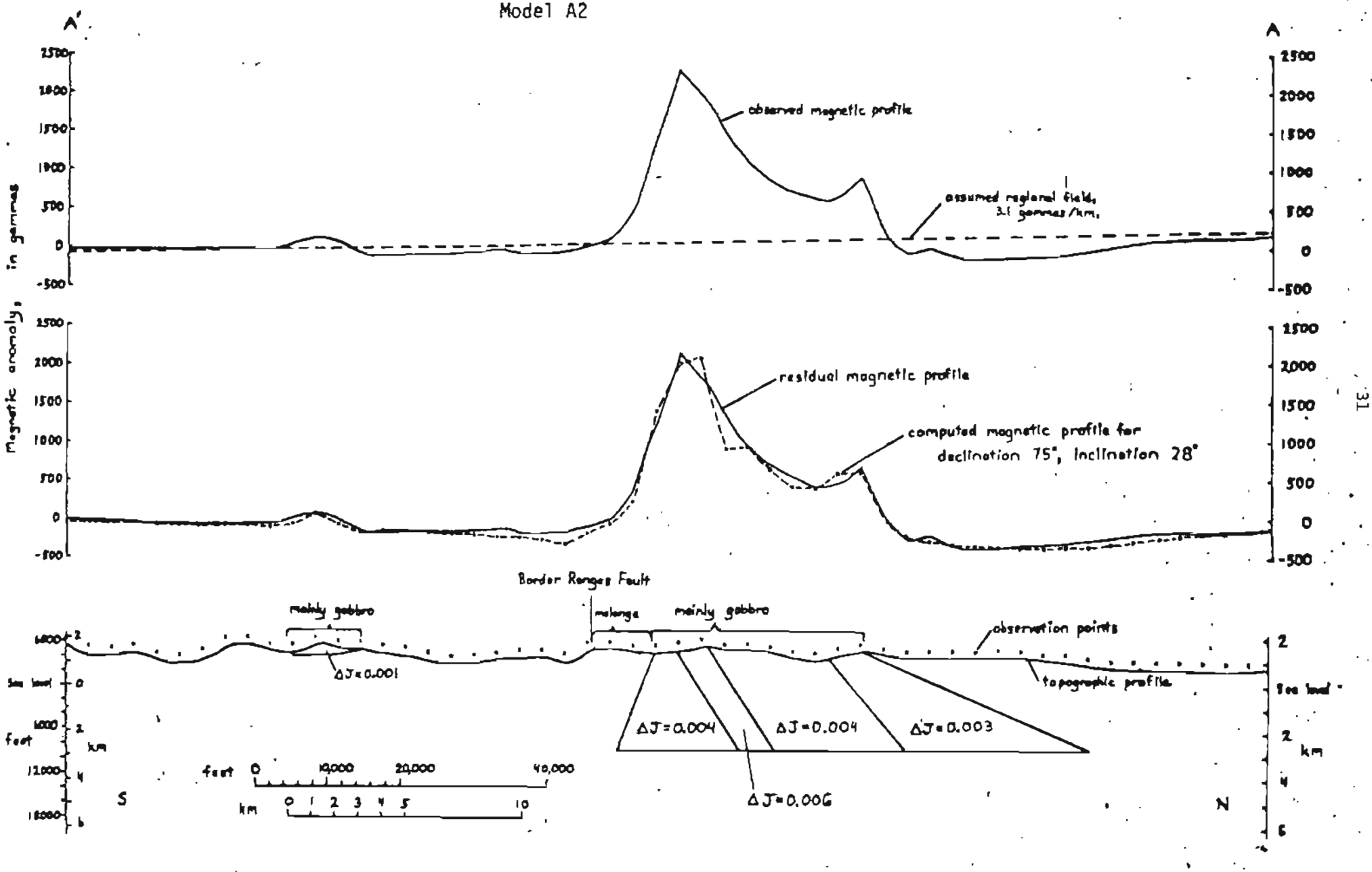

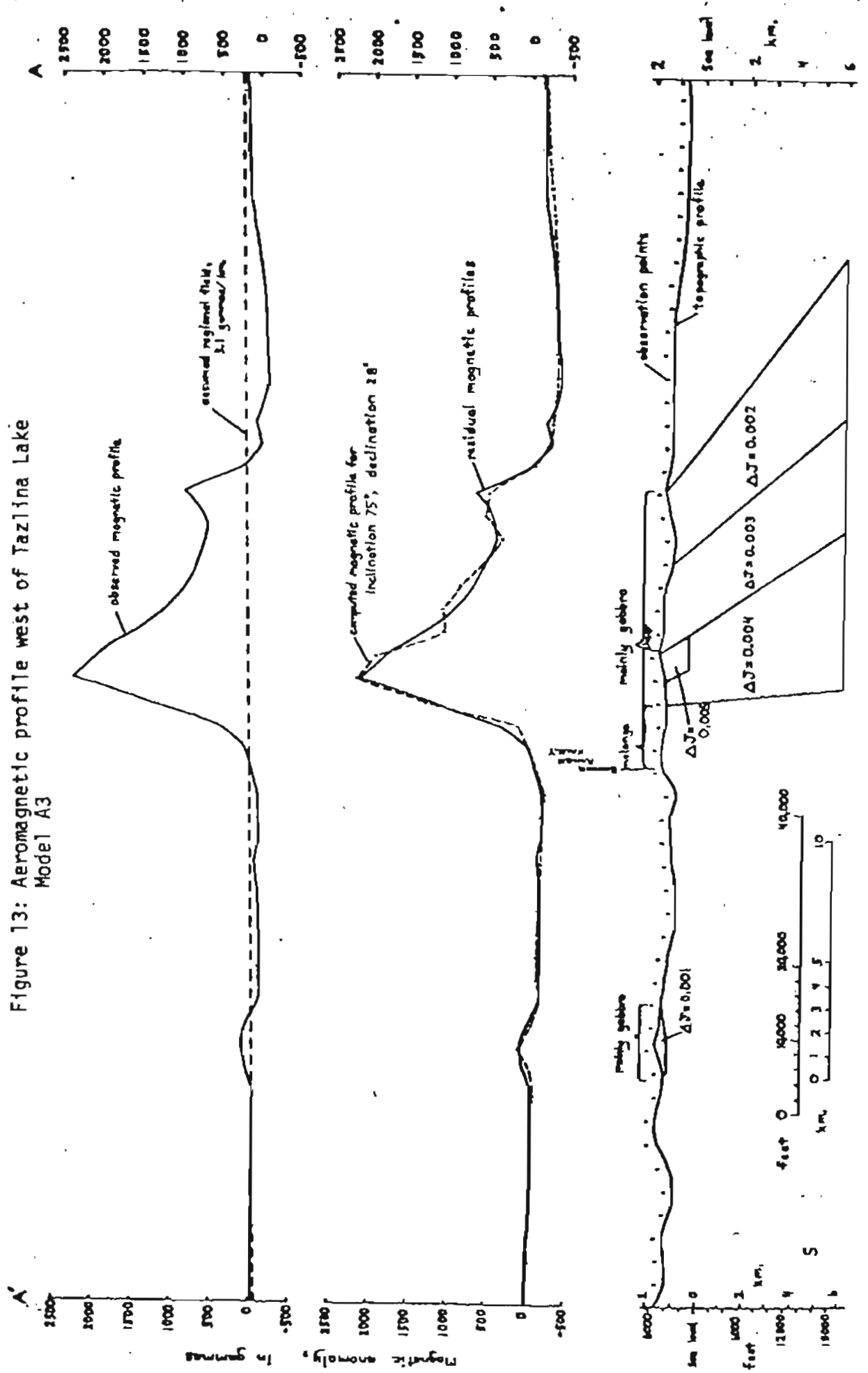

Figure 13: Aeromagnetic profile west of Tazlina Lake
Model A3

Figure 14: Aeromagnetic profile west of Tazlina Lake
Model B1

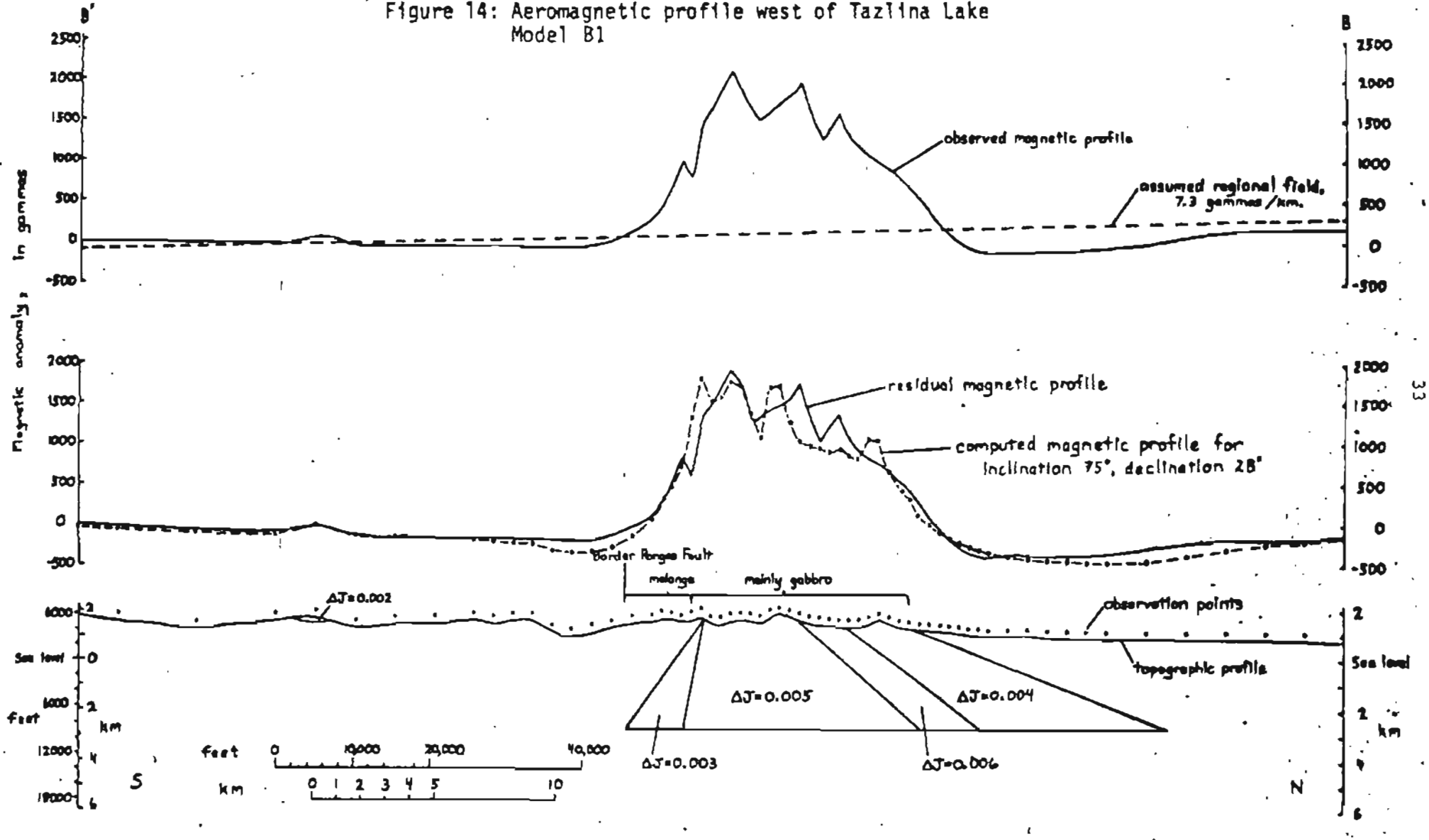

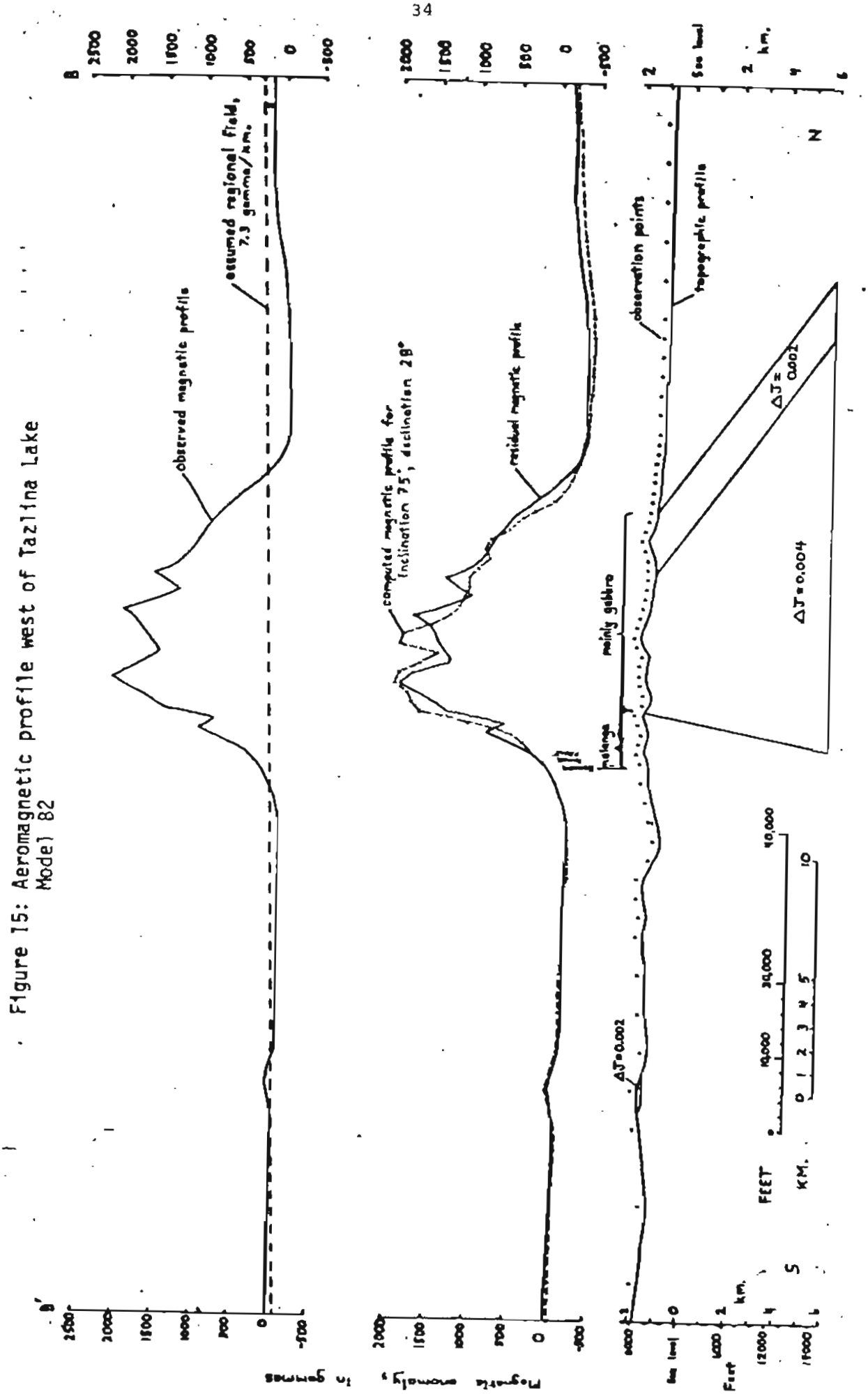

Figure 15: Aeromagnetic profile west of Tazlina Lake
Model 82

Figure 16: Aeromagnetic profile near Tazlina Lake
Model C1

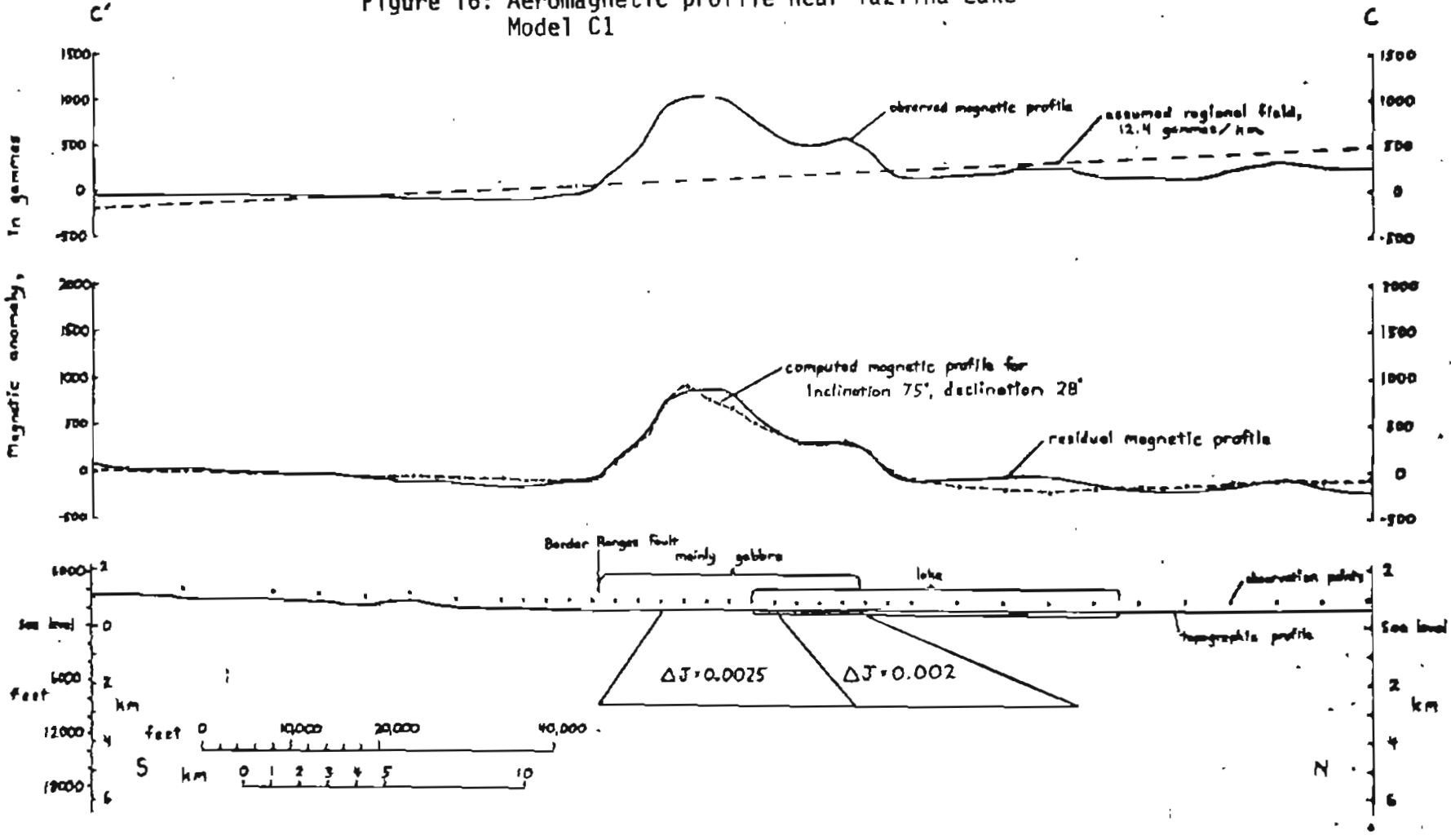

Figure 17: Aeromagnetic profile near Tazlina Lake
Model C2

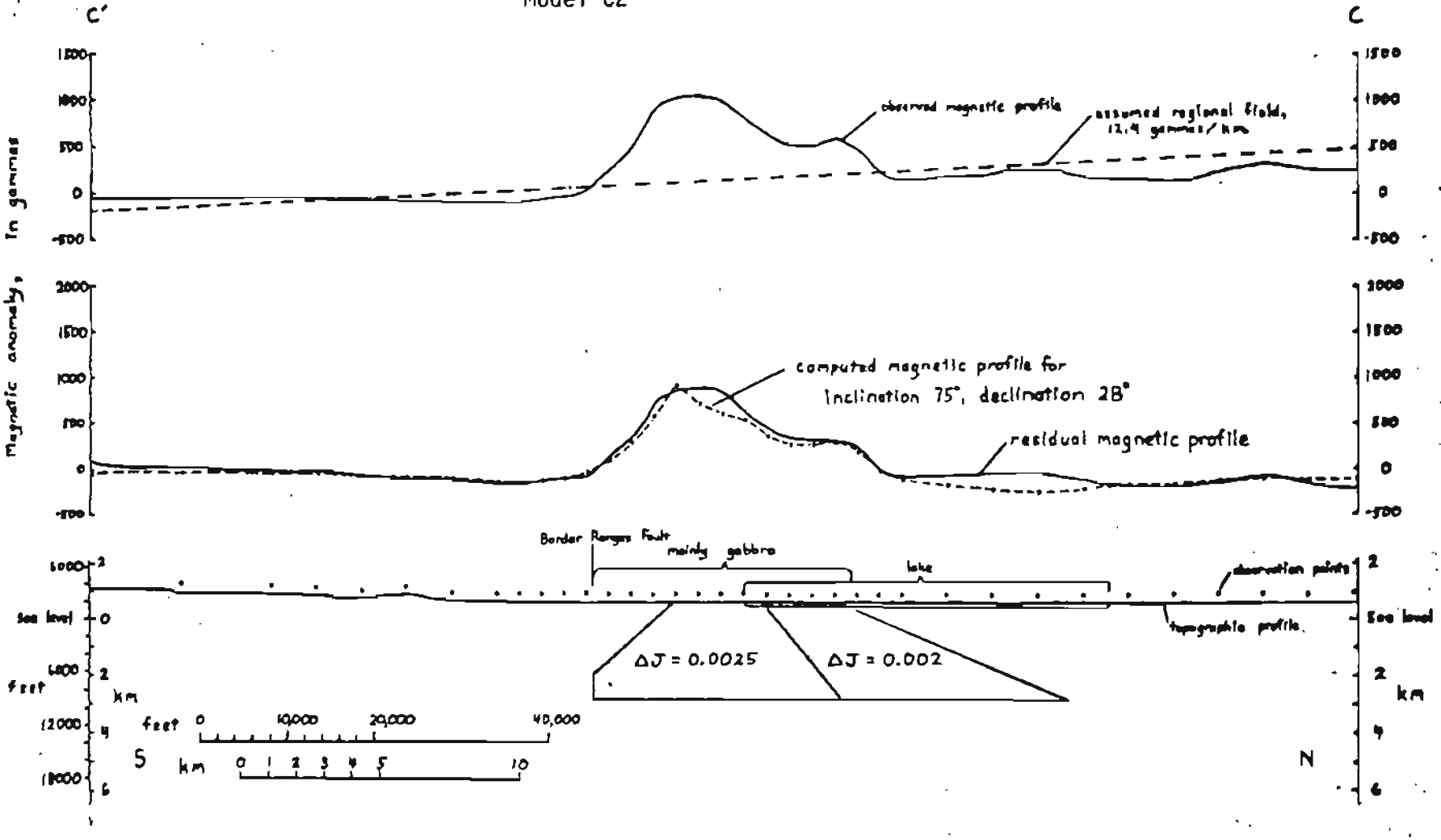

Figure 18: Aeromagnetic profile near Tazlina Lake
Model C3

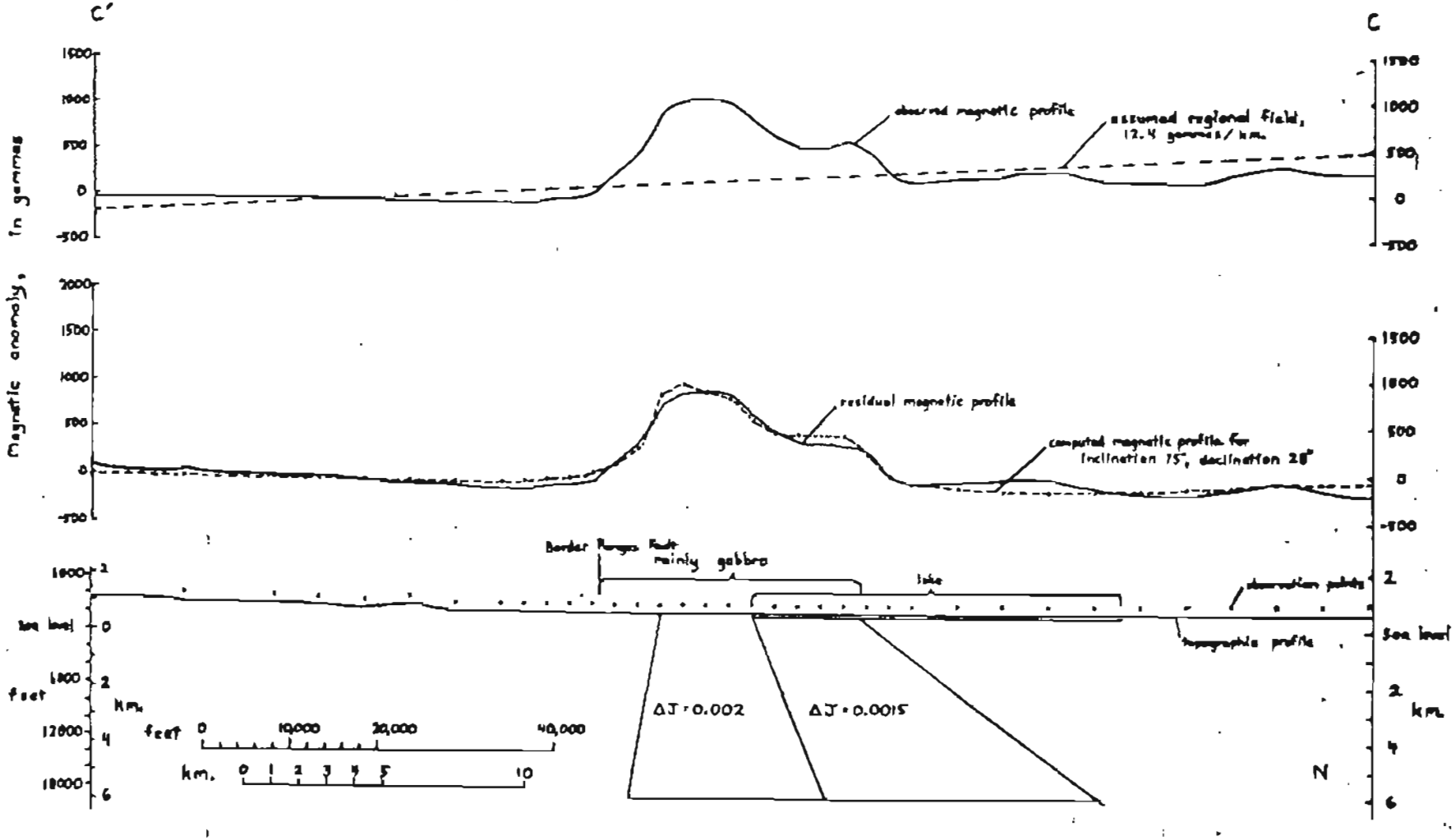

Figure 19: Aeromagnetic profile east of Tazlina Lake
Model D1

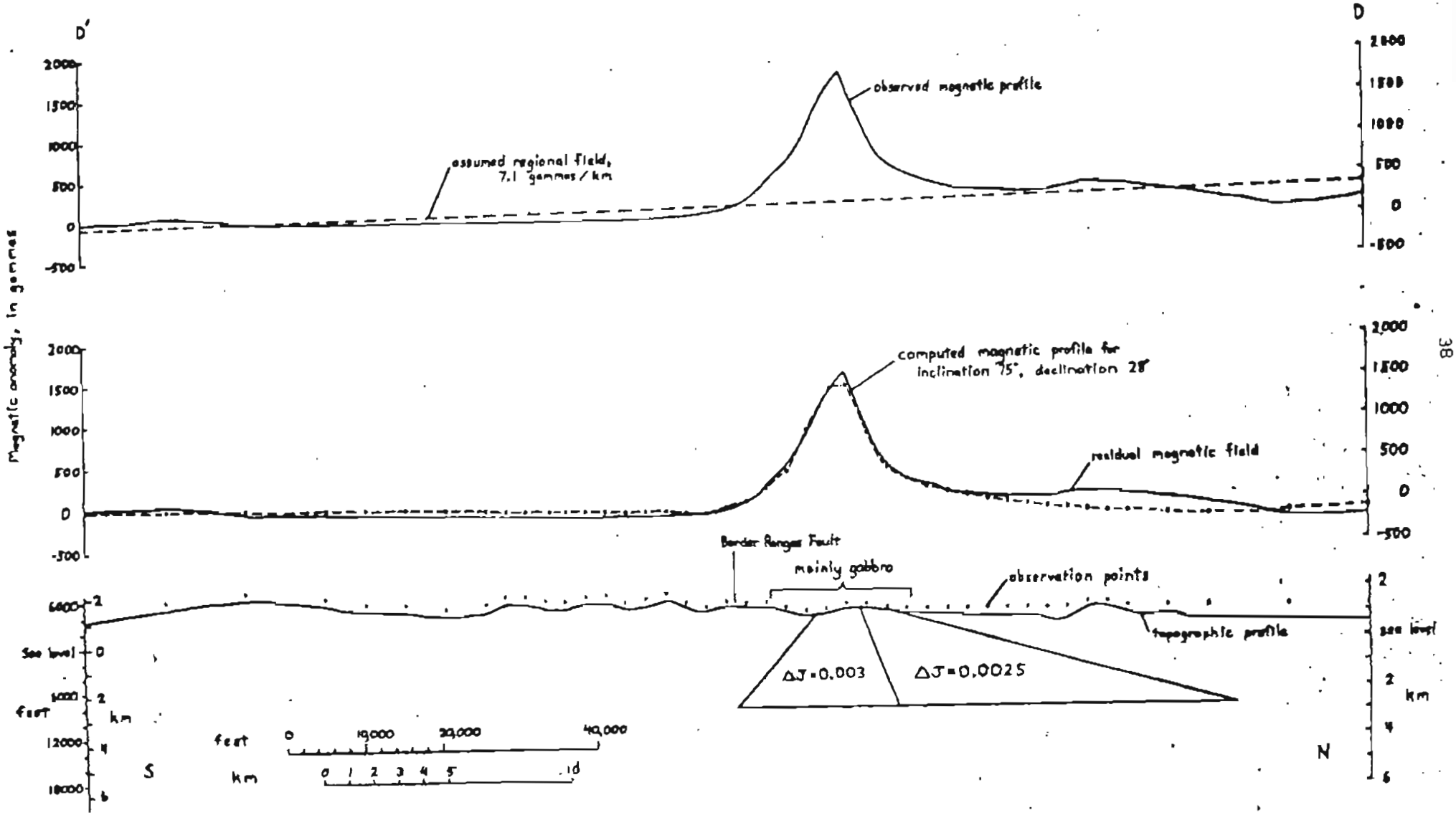

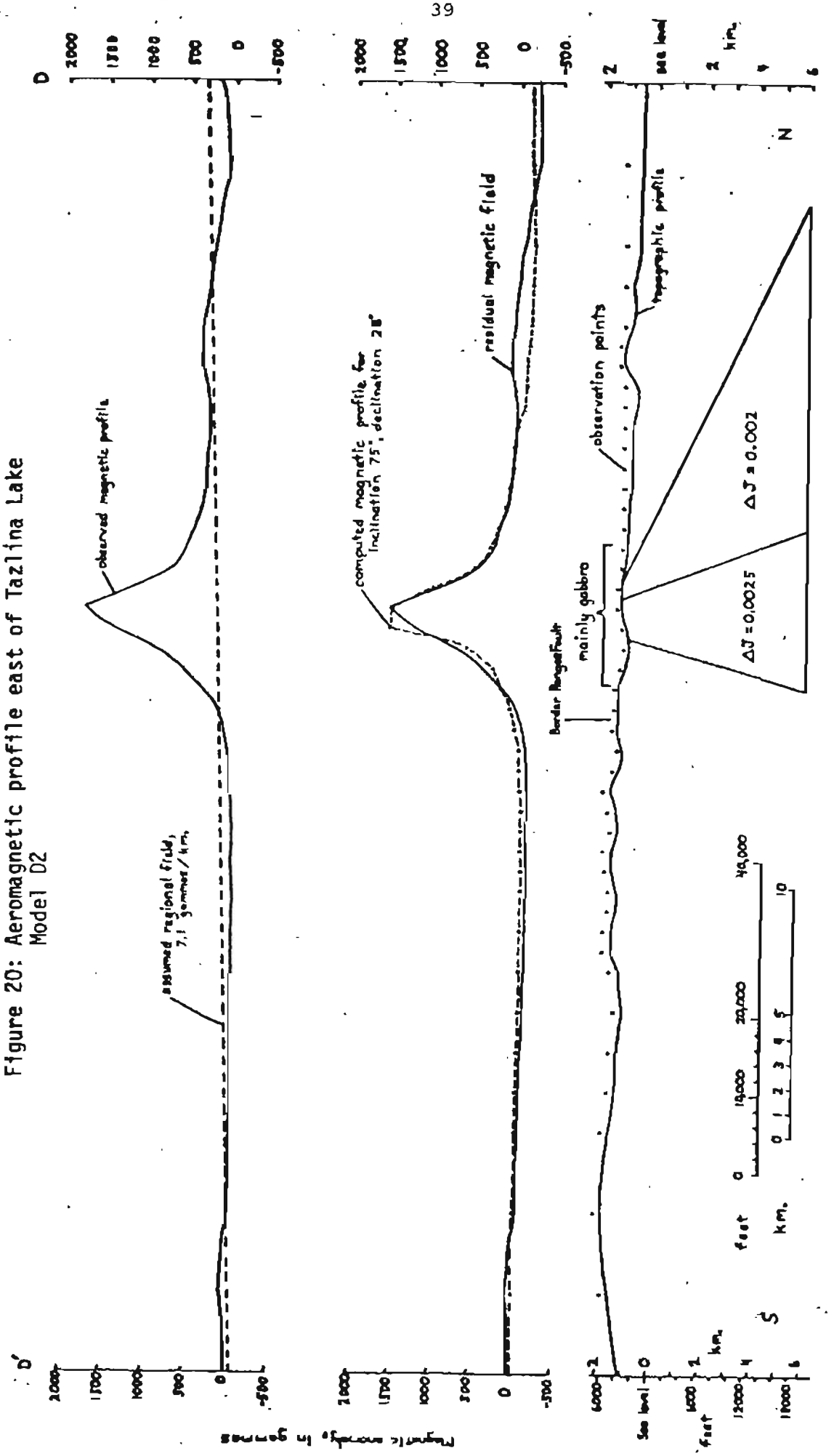

Figure 20: Aeromagnetic profile east of Tazlina Lake
Model D2

Figure 21: Aeromagnetic profile east of Tazlina Lake
Model E1

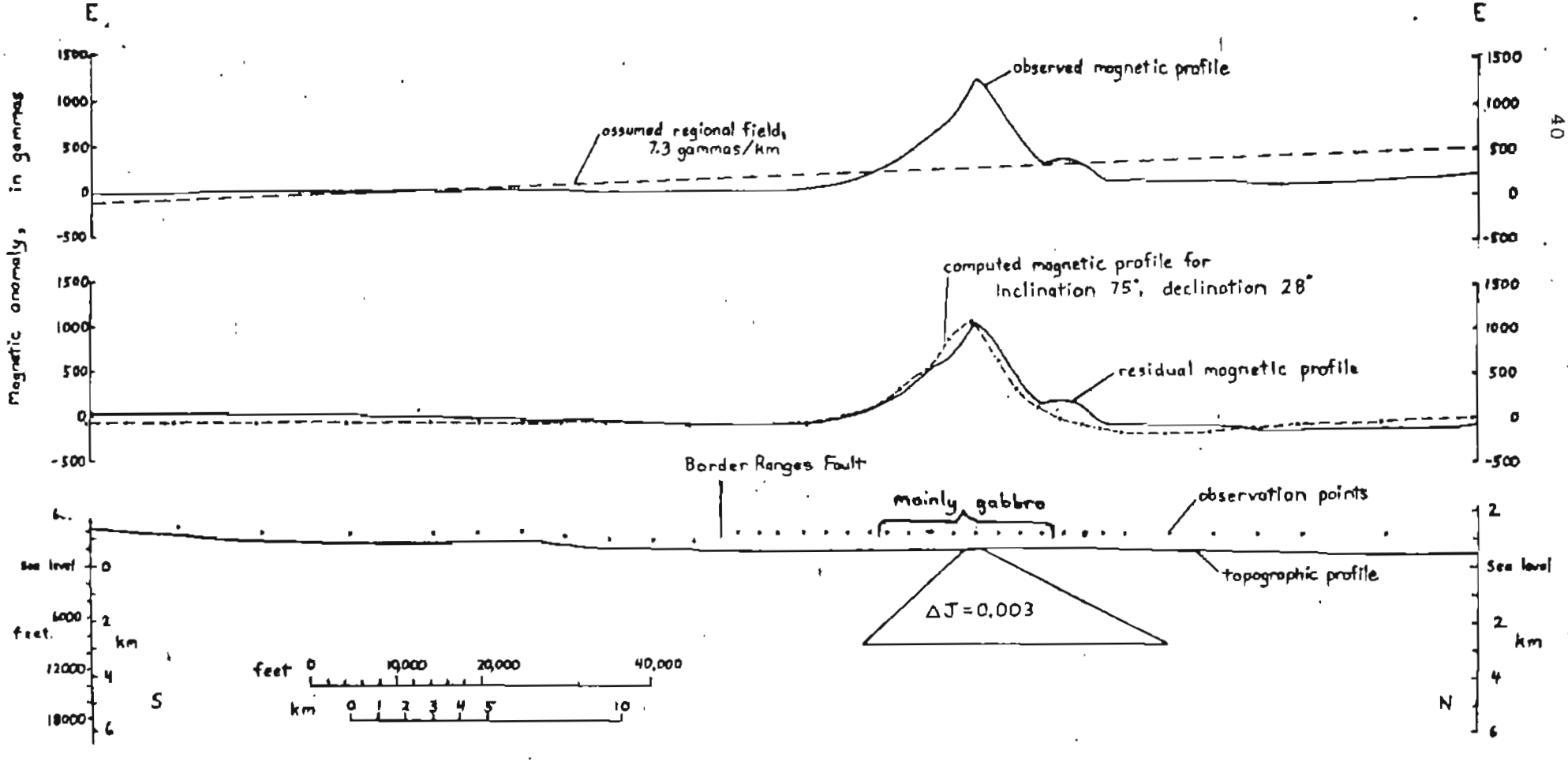

Figure 22: Aeromagnetic profile east of Tazlina Lake
Model E2

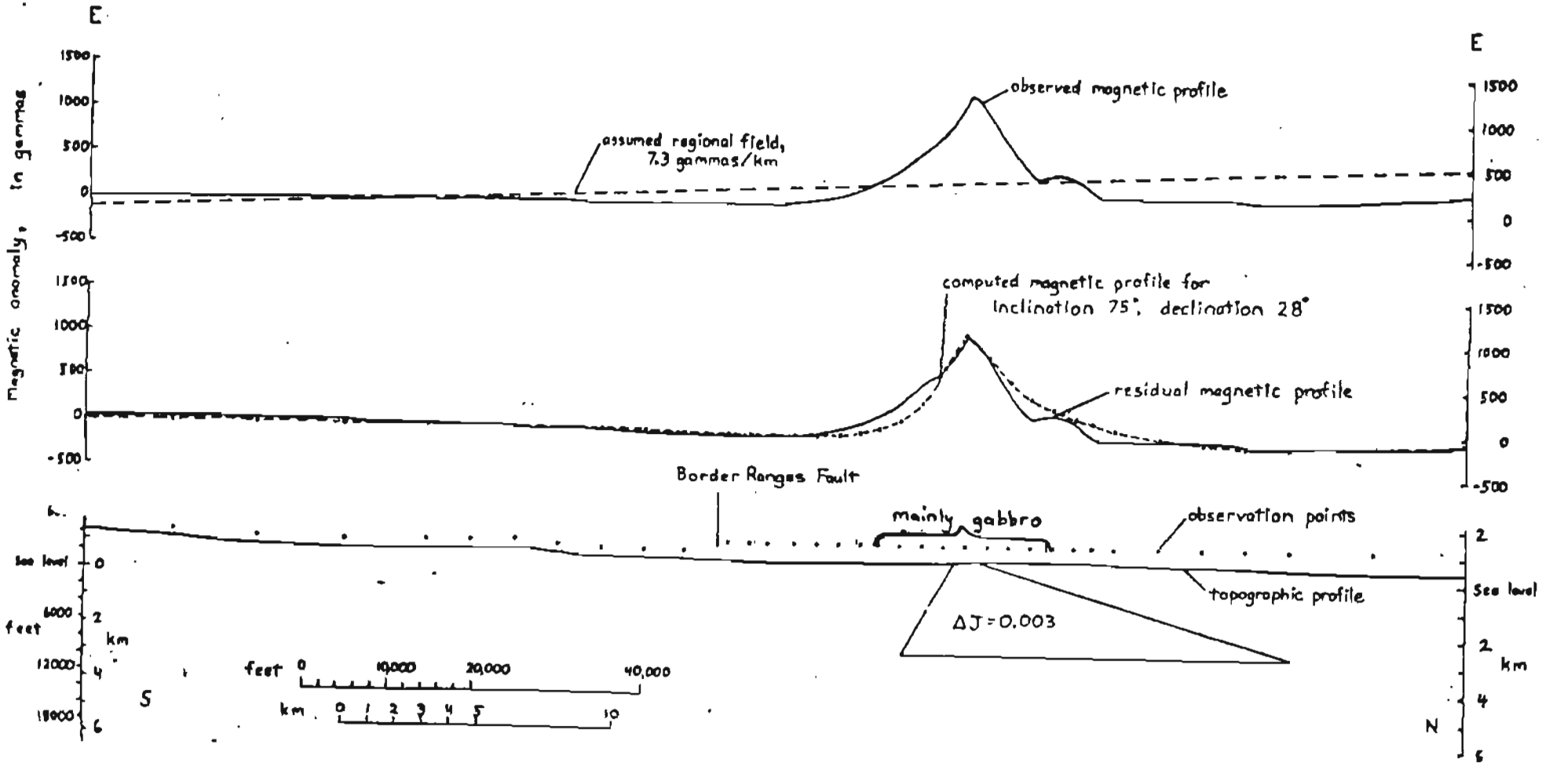

Figure 23: Aeromagnetic profile east of Tazlina Lake
Model E3

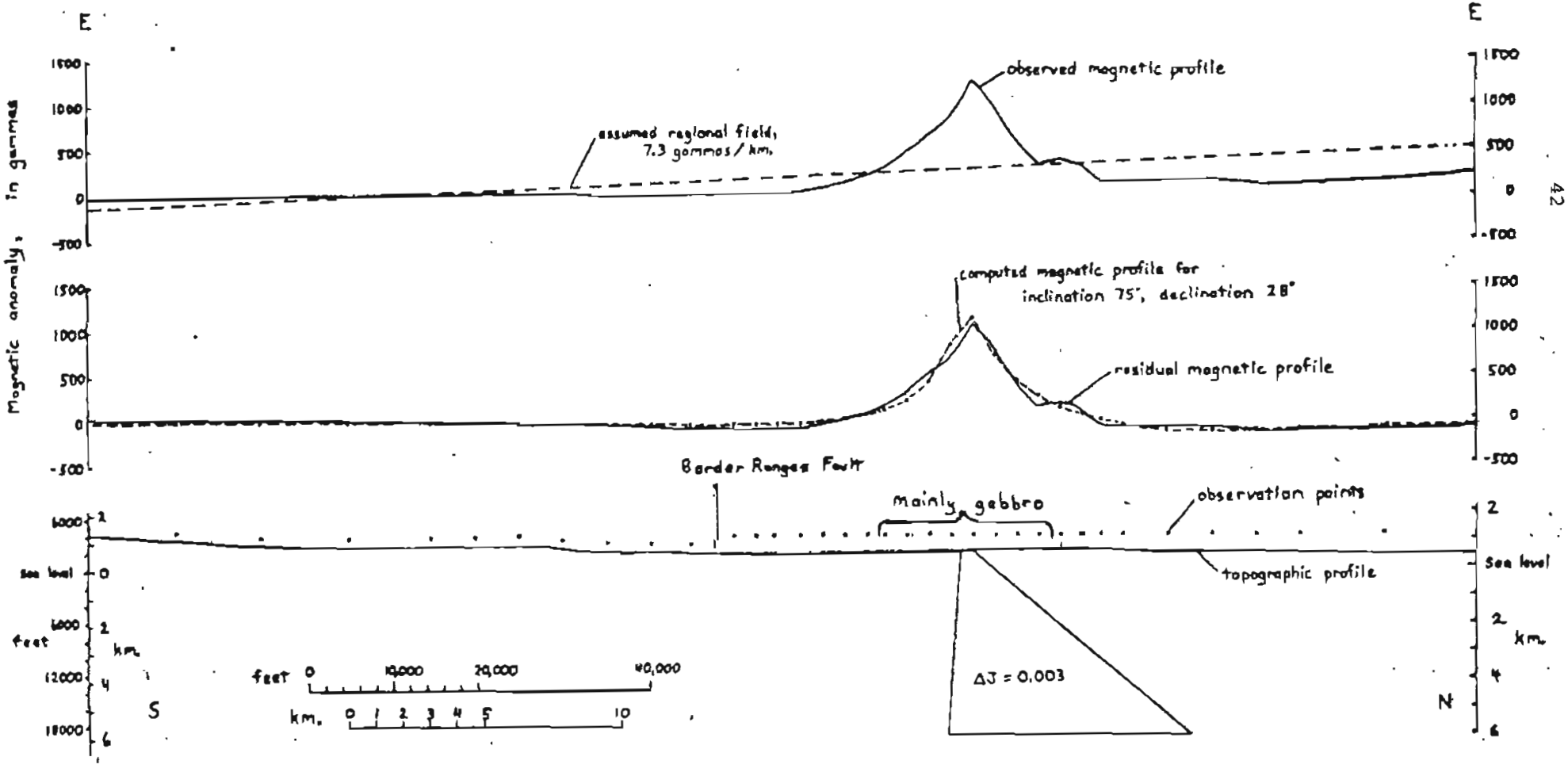

Figure 24: Aeromagnetic model with alternate directions of remanent declination and inclination; profile near Tazlina Lake

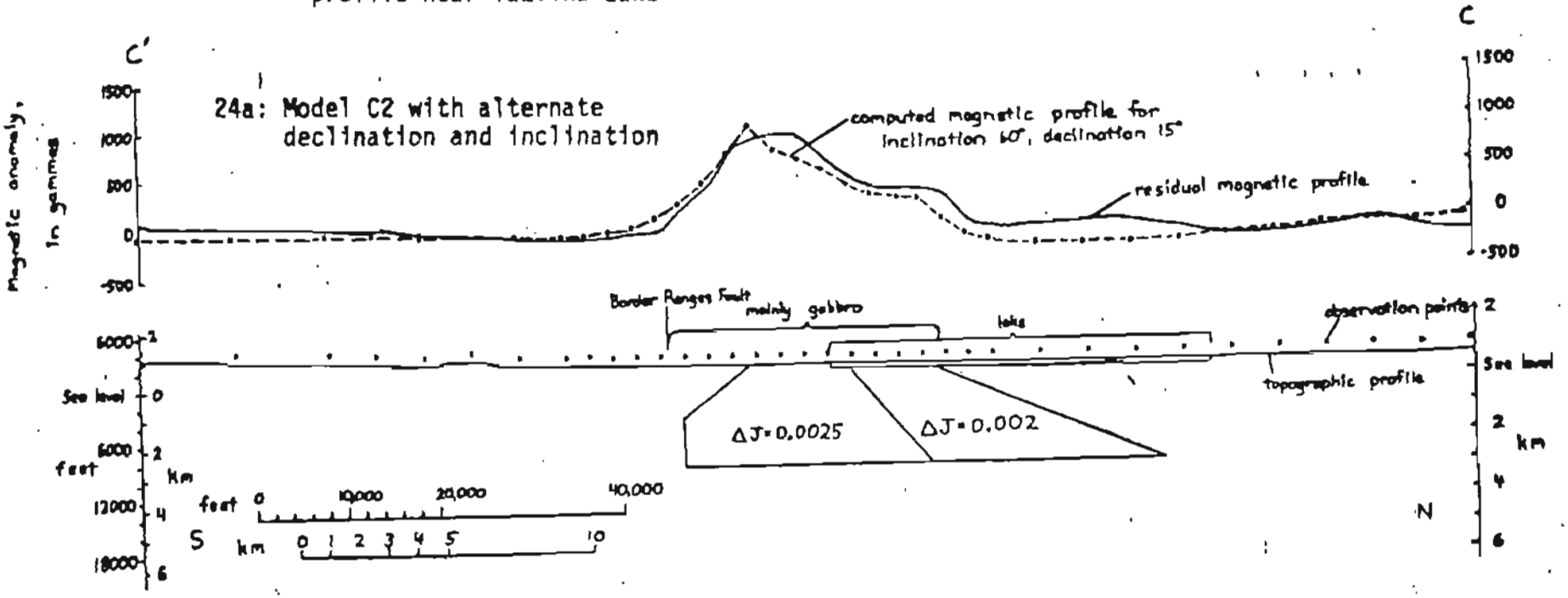

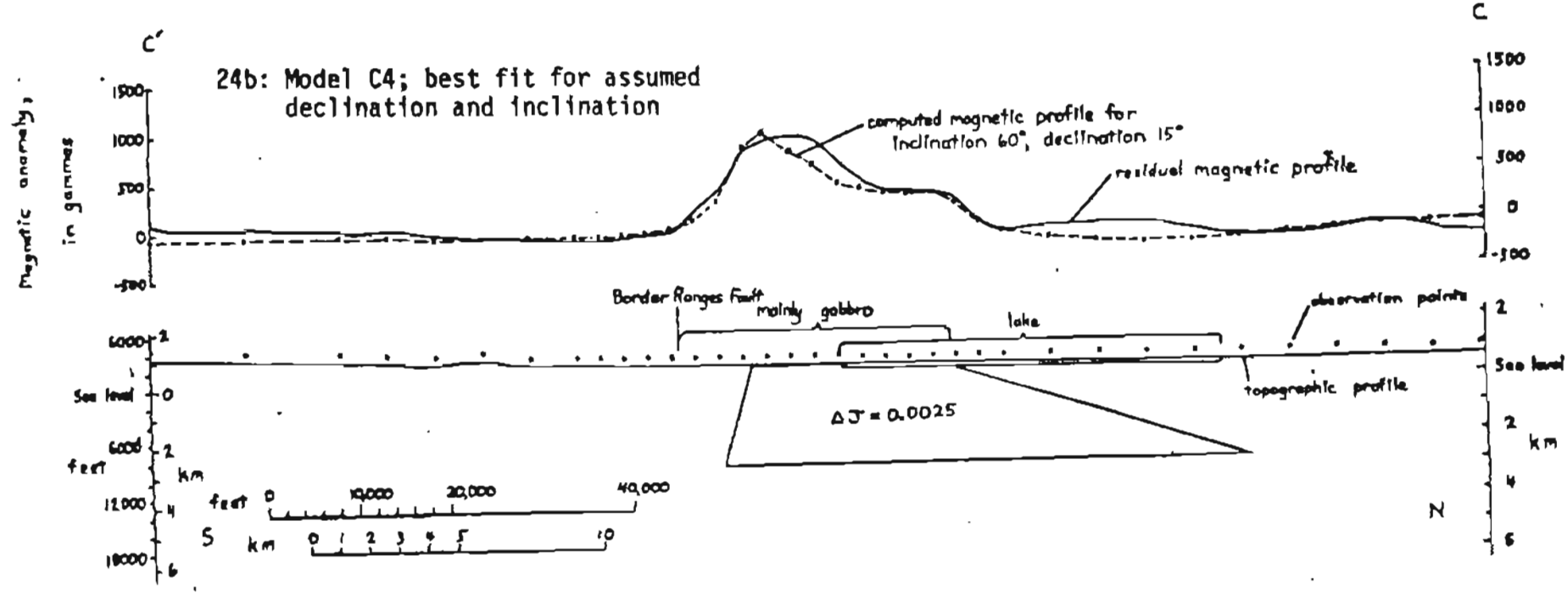

Figure 25: Aeromagnetic model with alternate directions of remanent declination and inclination; profile near Tazlina Lake

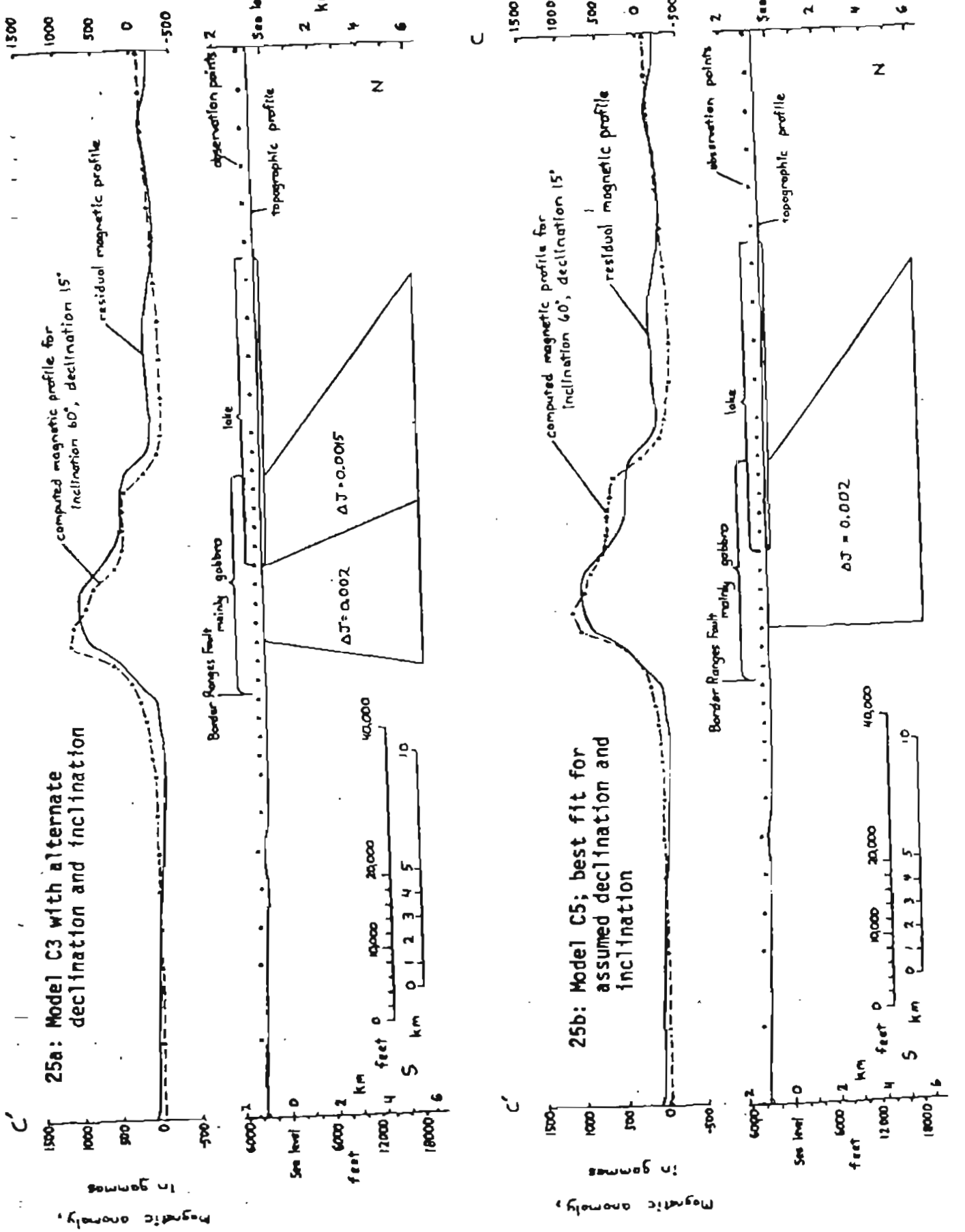

Figure 26: Aeromagnetic model with alternate directions of remanent declination and inclination; profile near Tazlina Lake
Model C6, best fit for assumed declination and inclination

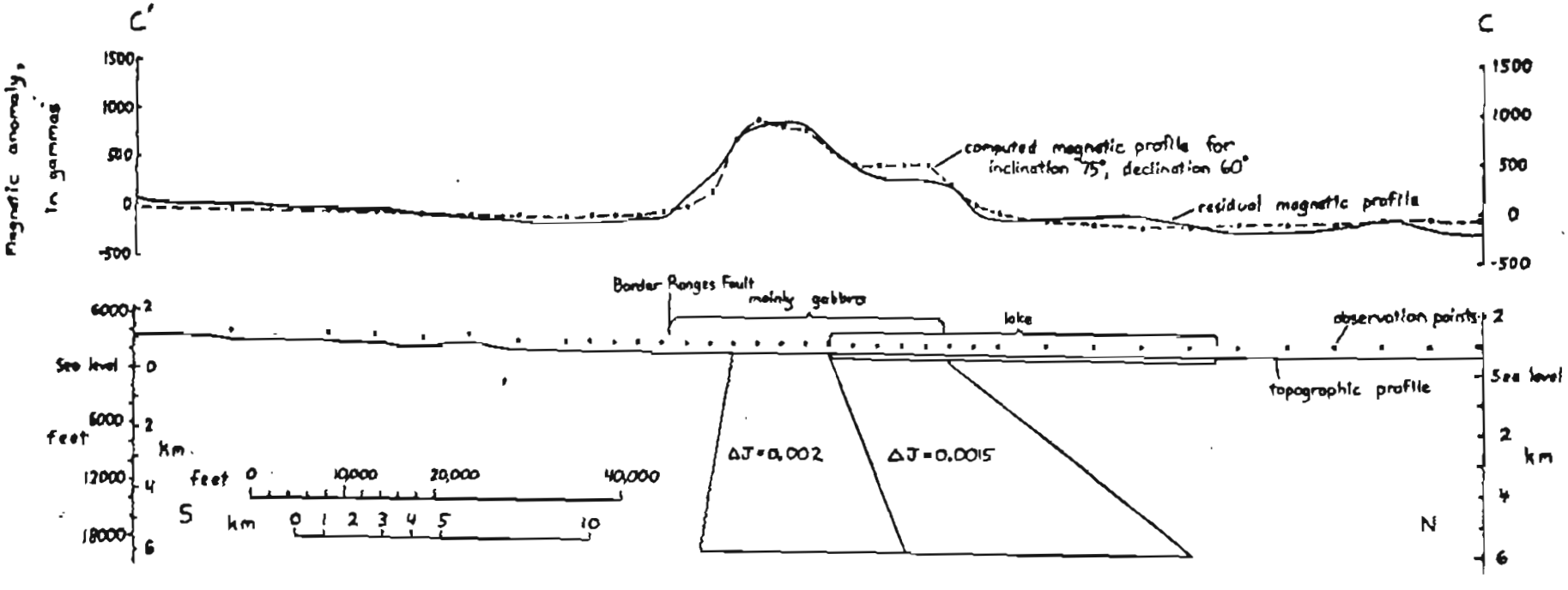

Figure 27: Diagrammatic sketch showing vertical fault between the gabbro body and volcanic rocks

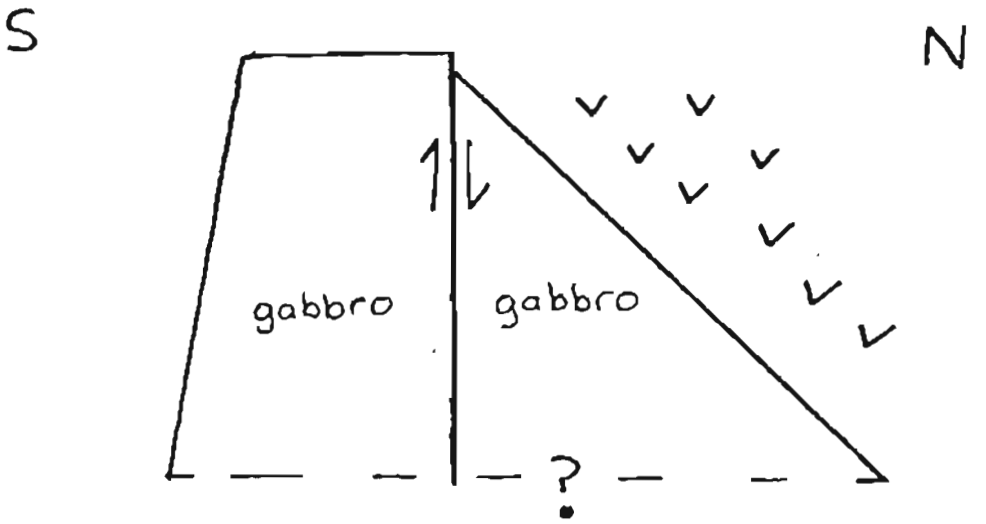

Figure 28: Diagrammatic sketch, showing alternative internal configurations of the gabbroic body

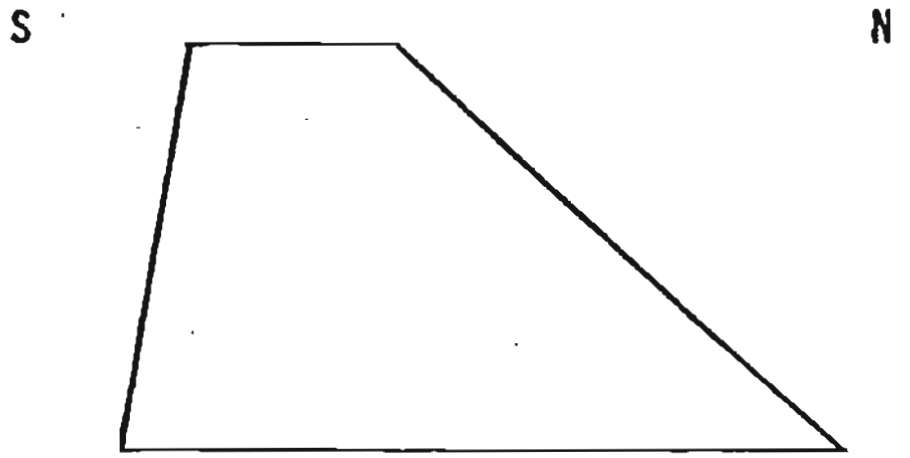

28a: Continuous mass of gabbro

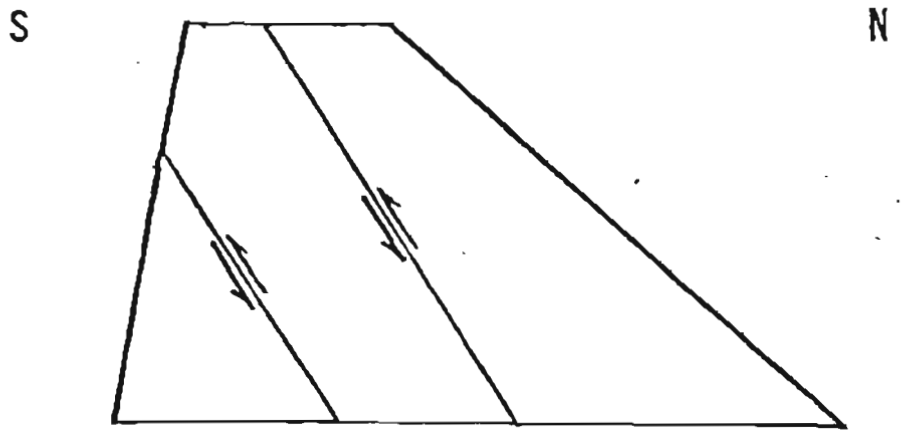

28b: Gabbroic body consisting of northward dipping thrust slices

Figure 29: Aeromagnetic profile of the Twin Lakes anomaly
Model F1

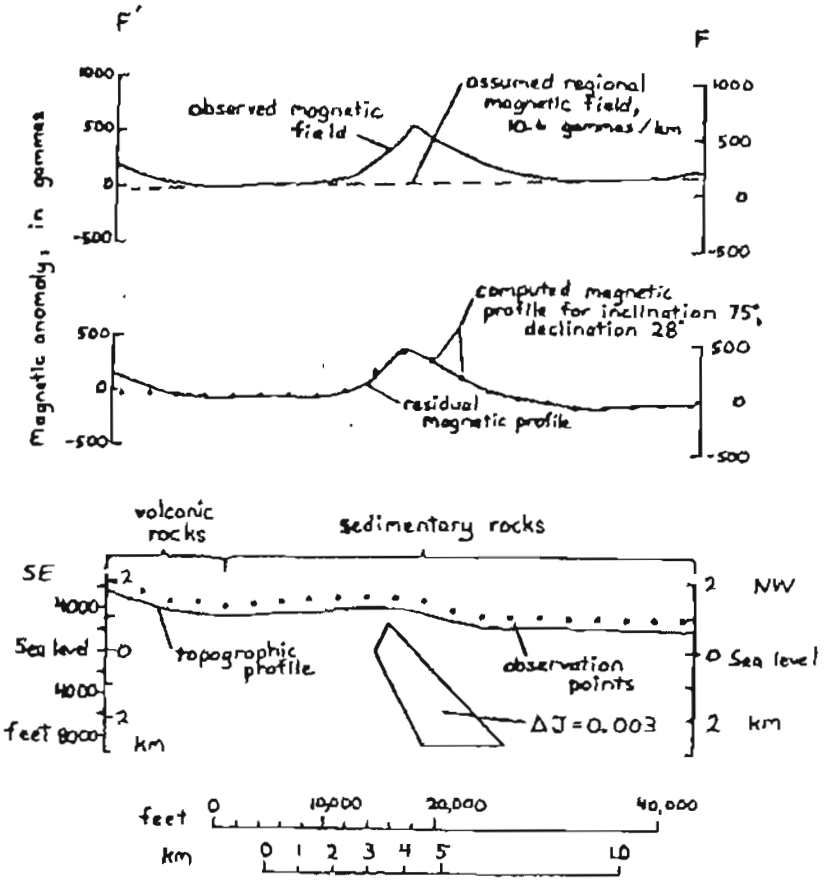

CONCLUSION

Geophysical modeling of the gabbro body provides information on the shape of the gabbro body, the possible dips of the surrounding contacts, the Border Ranges fault, variation of physical properties within the gabbro body, and delimits the prescence of ultramafic rocks.

The models imply that a north-south cross-section of the gabbro body is similar in shape to a trapezoid. The northern contact dips at low to moderate angles to the north, and the southern contact apparently dips steeply to the south. The attitude and depth of the base of the body is uncertain. Models with a horizontal base fit the observed gravity and aeromagnetic profiles and can extend to depths of three to eight km, or more, but other configurations for the base of the gabbro body will fit the observed anomalies equally well.

Two structural constraints on the geophysical models have been produced by the geologic mapping. The Border Ranges fault is steep to vertical, and the geophysical models do not need to violate this constraint. The northern contact, between the gabbro body and the volcanic rocks, is a steep to vertical fault zone. However, geophysical modeling indicates a shallow to moderate dip to the north for this contact. Unfortunately, a steep to vertical fault (separating mainly gabbro) will not show up in these geophysical models, fig. 27. Combining the geologic mapping and the geophysical models indicates that the gabbro was beneath the volcanic rocks, and a recent steeply-dipping to vertical fault moved part of the gabbro body to the surface, placing the gabbroic rocks in fault contact with the overlying volcanic rocks. The geophysical models indicate that gabbroic rocks exist below the volcanic rocks north of the exposed contact.

The southern contact of the gabbro appears to be steep and generally dips to the south. The internal configuration of the gabbro body can not be delineated by the geophysical models and the southward dipping gabbro may be composed of thrust slices dipping to the north, fig. 28.

The Border Ranges fault can be inferred to be steep to at least a depth of three km and probably more. The gabbro body appears to approach the Border Ranges fault at depth. Most of the observed anomalies imply that the gabbroic rocks extend southward to the Border Ranges fault; however, many models can fit the observed profiles and no definitive modeling of the Border Ranges fault is possible with the present data.

A decrease in the gravity and aeromagnetic anomalies to the east is most plausibly explained by an increasing amount of sedimentary rocks overlying the gabbro body. The presence of a more silicic phase of the gabbro in the eastern part of the survey area could also produce the observed geophysical anomalies. No major variations in rock type have been noticed as yet, as judged by geologic mapping, magnetic susceptibility measurements, and density determinations. However, geologic mapping is still reconnaissance in nature and few measurements on the physical properties on the rocks have been made. The present data is thus inconclusive.

Ultramafic rocks occur within the gabbro body. One mappable shear zone includes peridotites and tectonic blocks of serpentine (Winkler and others, 1981). Geologic mapping, the aeromagnetic map, and magnetic modeling indicate that this highly magnetic zone is approximately 45 km long, and crops out in the middle of the gabbro body west of Tazlina Lake. The shear zone is not apparent to the east of Tazlina Lake. To the west, the shear zone appears to

crop out at the northern edge of the gabbro body (Pessel and others, 1981). The absence of the northern section of gabbro in this area, may imply faulting, or just a normal variation of an intrusive contact.

Peridotites also crop out on the Nelchina River Valley. Gravity modeling indicates that the belt of ultramafic rocks is approximately 0.7 km wide. The lateral extent of these ultramafic rocks is not yet known, due to lack of detailed geological and geophysical data.

Source of the gabbroic body:

The source of this large gabbroic body is not known. The aeromagnetic and marine magnetic anomalies suggest that a mafic and ultramafic belt of rocks occurs on the northern side of the Border Ranges suture zone from at least the southern Copper River basin to southwest of Kodiak Island. Possible categories for the gabbroic rocks include ophiolites, a failed rift, the base of a primitive island arc, and an intrusion or series of intrusions.

The belt does not appear to be an ophiolite or a failed rift. The gabbroic belt does not appear to contain characteristic ophiolite sequences. However, the belt is structurally dismembered and an entire ophiolitic sequence would probably be difficult to find. Continental rifts are associated with alkali olivine basalt and tholeiitic basalts. The volcanic rocks in this area are dominantly andesitic in composition, and were presumably formed in an island arc. No rift-related volcanic rocks in this area are known.

The base of an island arc or some type of intrusion seems the most plausible explanation. The features of the base of an island arc are not known at this time. Clearly, the relationship of the gabbroic body to the volcanic rocks overlying the body is an important piece of evidence. Unfortunately, geologic mapping at this time is equivocal, and the geophysical models cannot determine whether the contact between the gabbro body and the volcanic rocks is intrusive or a fault. Though the exposed contact between the gabbro body and volcanic rocks is a fault, the shear zone may mask a an intrusive relationship. A possible intrusive relationship has been noted several times in the fault zone, but the contact has been equivocal. Two possible intrusions of the gabbroic rocks into the volcanic rocks have been noted in the western Valdez quadrangle. Detailed geologic mapping is required to determine the relationship between these two units.

Relationship of the melange zones and Border Ranges fault:

The steep Border Ranges fault does not appear to be the cause of the melange zone, as the two features possess markedly different styles of deformation. The Border Ranges fault is well exposed and appears to be a zone of steeply-dipping fault segments, whereas cataclastic deformation predominates north and south of the fault (in the gabbroic melange, the gabbro body, and the McHugh Complex). Furthermore, the gabbroic melange can be divided into several different map units, which trend into the Border Ranges fault west of the Nelchina River at an approximate angle of 20 degrees, and thus implies that the gabbroic melange was formed previous to the Border Ranges fault (Pessel and others, 1981).

The relatively unaltered gabbro body is the most obvious source for the gabbro blocks in the gabbroic melange. However, Winkler and others (1981) believe that the northern boundary of the melange zone should be termed the Border Ranges fault and that the crystalline melange is not related to the

gabbro, but is instead, an agglomeration of mafic rocks scraped off against the continental border during a subduction event. Resolution of this major controversy requires detailed geologic mapping and petrography to better understand the Border Ranges fault and suture zone.

ACKNOWLEDGMENTS

This research was undertaken in the summer of 1979 at the suggestion of G. H. Pessel, of the Alaska Division of Geological and Geophysical Surveys (ADGGS), who advised me and offered encouragement throughout the project. J. E. Case, of the U. S. Geological Survey (USGS), further encouraged the research and provided extensive advice. The research benefited greatly from many profitable discussions with G. Winkler (USGS), D. Barnes (USGS), and Professors N. H. Sleep, R. R. Compton, R. G. Coleman, and R. Lyon of Stanford University. Many others contributed to my knowledge of the area, notably A. Grantz, G. Plafker, T. Hudson, and D. L. Jones, all of the USGS. The manuscript was reviewed during many stages of preparation by G. H. Pessel, N. H. Sleep, and R. J. J. Newberry. R. J. J. Newberry also supplied advice and manual labor for the assemblage of the maps and figures.

Geologic mapping was supported by the ADGGS, and geophysical modeling was supported by the USGS, and was partly funded by National Science Foundation grant EAR80-01078. Both surveys supplied geophysical data and geologic maps.

To all of the above individuals and organizations I am deeply grateful. Many others contributed to my knowledge of the area, but are too numerous to be mentioned by name.

APPENDICES
MEASUREMENTS, PROPERTIES, AND COMPUTATIONS

APPENDIX A: GRAVITY DATA AND COMPUTATIONS

The gravity stations used for modeling and contour maps are from composite sources. During 1979 and 1980, 105 gravity stations were established in the northeast corner of the Anchorage quadrangle, between W. long 147° 00' to 147° 40' W. long., and 60° 30' to 61° 50' N. lat., by the Alaska Division of Geological and Geophysical Surveys. During the past 30 years, approximately 300 stations, including a Tazlina Lake traverse and 30 stations in 1979 were established by the United States Geological Survey in the area.

Three LaCoste and Romberg gravity meters were used to established the 1979 and 1980 stations. All meters appeared to be functioning correctly, and were checked against an established U. S. G. S. calibration loop in Anchorage and California. Most of the gravity measurements previous to 1979 were made with World Wide meters.

The data was tied into the main gravity network by looping field base stations with established gravity bases on the Glenn Highway. Several field base stations were used during the project. Gravity stations were established with looped traverses which were generaly closed within a four hour period. No traverses had a greater time lapse than ten hours.

Locations and Elevations:

Elevation control was established from map locations and altimeter readings. The altimeters were checked with bench marks for accuracy and functioned correctly. The altimeter readings were given priority in discrepancies between map and altimetry elevations.

The Tazlina Lake gravity traverse has an additional source of error due to the unknown depth of Tazlina Lake and its related sedimentary rocks. Depth sounds were made in 1952 by John Williams, of the U. S. G. S. Several models were tried with lake depths ranging from approximately 45 to 120 m. No major changes in the shape of the gabbro body occurred.

Reduction of gravity data:

The gravity data presented in this paper have been reduced by computer techniques. Reduction of the gravity data was also computed by hand to insure that the computer program worked correctly. Only minor discrepancies, less than 0.7 mgal (milligal) were found, and were due to different methods of averaging the temperature measurements established at the gravity stations. Simple Bouguer corrections using a uniform density of 2.67 g/cm^3 (grams per cubic centimeter) were made for all stations. The bouguer anomalies were compiled as a contour map having a five milligal contour interval, plate 2. The simple Bouguer values are estimated to be correct to +/- 2 mgals. Uncertainties in elevation and location of the gravity stations are the main source for the error.

Various minor corrections were made to the data before computing the

simple Bouguer anomaly. The meter constant from a LaCoste Romberg table was applied, linear drift was assumed, and the data normalized, and a correction factor to the altimetry was applied for changes in relative humidity.

The following standard equations were used:

1. Simple Bouguer anomaly with reduction density of 2.67 g/cm^3.

$$\Delta g_b + (0.003086 - 200\pi G\rho)h - g_\gamma$$

where Δg_b = simple bouguer anomaly
h = height in feet above sea level
π = 3.1415...
ρ = density constant, assumed value of 2.67 g/cm^3
G = gravitational constant
g_γ = latitude correction

Latitude correction was computed according to the 1967 formula;

$$978.03185(1 + 0.005279905 \sin^2 \vartheta + 0.000023462 \sin^4 \vartheta)$$

2. Complete Bouguer anomaly

$$\Delta g_{cba} = \Delta g_b + t.\ c.$$

where g_{cba} = complete Bouguer anomaly
t. c. = terrain corrections computed to 50 km

Terrain corrections:

Terrain corrections to 50 kilometers were made for the two modeled gravity profiles, fig. 30. The Nelchina gravity stations were terrain-corrected by hand and computer, and the Tazlina gravity stations were terrain-corrected by hand. The Nelchina profile generally has larger terrain corrections than the Tazlina Lake profile, due to the rugged topography near the Nelchina glacier. The terrain corrections on the Nelchina were less than 11.0 mgals, with the majority of terrain corrections being between 5 and 9 mgals, see fig. 30. All terrain corrections and on the Tazlina Lake profiles were less than 10.0 mgals, with the majority being less than 5 mgals. The terrain corrections are assumed to be accurate to +/- 2.0 mgal for most stations and +/- 4 mgals for the least accurately located stations.

The gravity values shown in the profiles to the south and north of the established gravity stations were interpolated from Barnes (1979). The error associated with the terrane corrections for the northern values is approximately +/- 3 mgals, due to interpolation and estimation. The values in the Chugach Mountains have a larger error, possibly up to +/- 10 mgals, due to interpolation between the few gravity stations and the rugged terrain.

Assumed regional gravity field:

Simple Bouguer values were interpreted from a regional gravity map of the area (Barnes, 1979). An approximately constant regional gravity field was assumed for the modeled profiles, as the difference between the estimated complete Bouguer values north and south of the gabbro body are generally less than +/- 5 mgals.

Rock Density:

Density measurements from this study and from Case and others (1979b) were used for modeling, see table 3. The average density of the gabbro body, 2.92 g/cm^3 was sufficiently distinct from the densities of the adjacent rock belts, generally 2.72 g/cm^3, to allow modeling of the gravity profiles. However, the number of samples measured in a few of the units is not statistically valid. The densities measured and used are appropriate values for the corresponding rock type.

Program used:

A program assuming two dimensional structures was used (U. S. G. S. program 2dgrav3, C. Roberts, 1977). The structures, including rock formations, glaciers, and lakes, are assumed to extend to infinity in both directions in this program. This assumption will not introduce much error as the gabbro body is thin in outcrop relative to its length and is the dominant contributor to the gravity anomaly. The gravity models were plotted at right angles to the geologic trends, to minimize the errors.

Figure 30: Histogram showing values of Terrain corrections for the two gravity profiles

(50 km radius employed for terrain corrections)

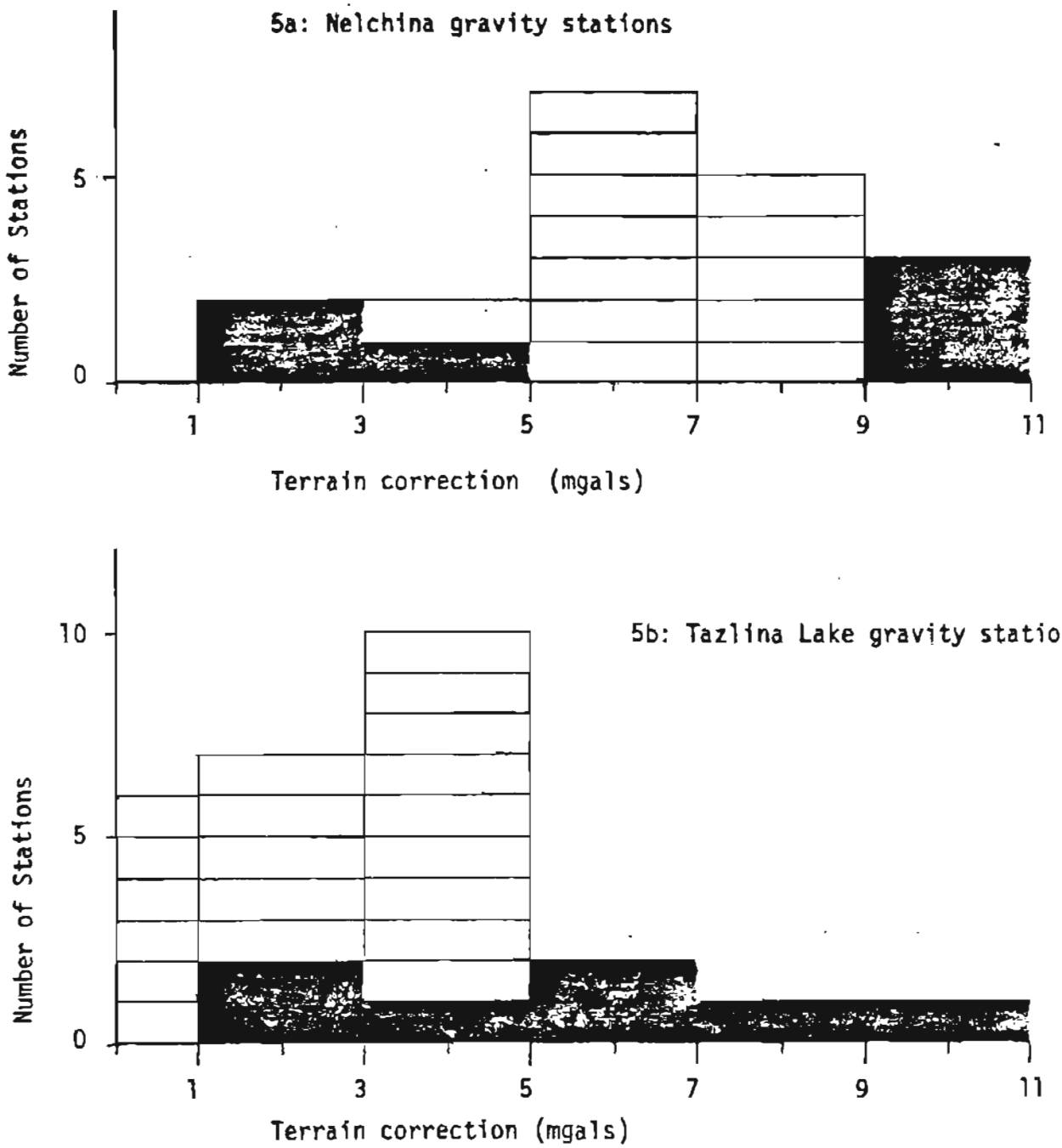

Note: solid blocks indicate terrain corrections on values interpolated from plate 2

TABLE 3.

DENSITY DETERMINATIONS

ROCK TYPE	NO. OF SAMPLES	DENSITY (gm/cubic cm) MIN.	MAX.	AVE.
Sedimentary and metamorphic rocks of the Orca and Valdez Group	113*	2.67	3.04	2.78
McHugh Complex	35	2.62	3.14	2.79
Talkeetna Formation	14	2.61	2.90	2.72
Gabbro belt	72	2.68	3.22	2.92

* 105 samples from Case et al. (1979)

APPENDIX B: AEROMAGNETIC DATA AND COMPUTATIONS

Aeromagnetic Maps:

Aeromagnetic reconnaissance of the majority of the Valdez quadrangle was flown and compiled by LKB Resources, Inc. in 1978. In addition, the northernmost part of the Valdez quadrangle was flown in 1954 and 1955 and compiled in 1958 by Andreason and others. Neither map covers the entire gabbro body in the Valdez quadrangle and the 1958 aeromagnetic map is therefore spliced into the 1978 map (plate 3). Some uncertainty, approximately +/- 50 gammas, is associated when combining the two aeromagnetic maps. Unfortunately, the northeastern corner of the Anchorage quadrangle is not covered by aeromagnetic data.

The 1978 aeromagnetic survey was made with a fluxgate magnetometer installed in a fixed-wing aircraft. Total intensity magnetic data were recorded along 64 north-south and 54 northeast-southwest flight lines. The flight lines, approximately 1.6 km. apart, were flown drape style, 300 meters above the terrain.

The original survey, in 1954, covers a portion of the current survey and a large area to the north of this survey, the Copper River basin. The 36 flight lines were flown at 1.2 km barometric pressure, except where terrain interfered and were spaced 1.6 km. apart. The aeromagnetic profiles in the 1958 survey were flown at a barometric flight elevation of 1.2 km, except locally where topography required higher flight elevations. Continuous total-intensity magnetic data along flight traverses were obtained from a modified AN/ASQ-3A airborne magnetometer. A detecting element was towed about 23 meters below the aircraft.

The aeromagnetic maps are joined and contoured, plate 3, at 100 gamma intervals over the gabbro body and 20 gamma intervals elsewhere. Joining the aeromagnetic maps introduces error, approximately +/- 50 gammas. 50 gammas is well within the uncertainties is the original aeromagnetic data. Two profiles, D and E, are compiled from the combination of aeromagnetic maps.

Generalization of magnetic character:

The simplicity of the models is probably the largest source of uncertainty, particularly in the magnetic models. The recording instrument for magnetic intensity is placed far above the magnetic body for aeromagnetic surveys. The magnetic effects of a number of closely spaced sources will blend together when viewed from a large distance and will appear as a single anomaly pattern. Thus, it is impossible to sort out different magnetic bands when using only aeromagnetic data.

The magnetization of the gabbro body appears to vary considerably between neighboring outcrops. Magnetic susceptibility measurements indicate a change of magnetization on the order of delta J=0.003 for adjacent outcrops. Unfortunately, the number of susceptibility measurements are too few to delineate magnetic zones within the gabbro body, and the magnetic properties of the gabbro body at depth are not known. Several large blocks with differing magnetizations are combined in most of the aeromagnetic models. Large magnetic blocks consisting of uniformly magnetized material are an unlikely occurrence in this gabbro body. The models shown in this paper are the simplest models that approximately fit the observed profiles. The gravity models

are also a product of simplification.

Remanent and induced magnetism:

Gabbro body: A plot of the susceptibilities (K) of 59 specimens from the gabbro belt shows the median susceptibility value to be 4.4 X 10 -3 emu/cm^3, fig. 31. The induced magnetism (Ji) in the Earth's field (F), 0.52 Oe at 62 N. lat., is

$$Ji = KF = 4.4 \times 10^{-3} \times 0.52$$
$$= 2.3 \times 10^{-3} .$$

Magnetizations used in the modeled profiles C, D, and E generally differ from Ji only by 0.7 X 10 -3 emu/cm^3 or less. Aeromagnetic profiles A and B cross a belt of high magnetic susceptibility and the magnetizations used in the models were higher, up to 6.0 X 10 -3.

The magnitude of the remanent magnetization of 18 specimens from the gabbro belt had a median value of 2.8 X 10 -3, table 4. No oriented samples were taken. Demagnetization in an alternating field implied that the remanent magnetism is soft, fig. 32. Alternative declinations, within 60 degrees of the present magnetic field, and inclinations for the remanent magnetic field were modeled in several magnetic profiles. The dips of the contacts did not change more than 10 degrees.

Three specimens of serpentinite from the gabbroic melange zone were tested for magnetic susceptibility, and produced values of K = 0.0000, 0.0005, and 0.0007 emu/cm^3. The aeromagnetic anomaly over the gabbroic melange is low and the assumption that the gabbroic melange is too sheared to be magnetic is probably valid (implying weathering of magnetite to ferric oxide, such as hematite).

Surrounding rocks:

The magnetization of the rocks surrounding the gabbro body was neglected in the models. The metasedimentary rocks to the south of the gabbro belt have virtually no magnetic susceptibility, as measurements from Case and others (1979b) and from this study indicate. 28 samples from the McHugh Complex were measured in this study, and only one sample, a marble, had a magnetic susceptibility greater than 0.0005 emu/ cm^3, fig. 16.

Susceptibilities of 14 volcanic rocks from the Talkeetna Formation to the north of the gabbro were measured and show a median susceptibility of K=0.0011 emu/cm^3, fig. 16. Though the number of specimens measured is not statistically valid, inspection of the aeromagnetic map indicates that the a magnetic low, in contrast, is generally associated with the volcanic rocks of the Talkeetna Formation. Neglecting the magnetizations of the volcanic rocks and the metasedimentary rocks is probably valid for the purposes of these models.

Assumed regional magnetic field:

Figure 31:Histogram of Magnetic Susceptibility (K) measurements

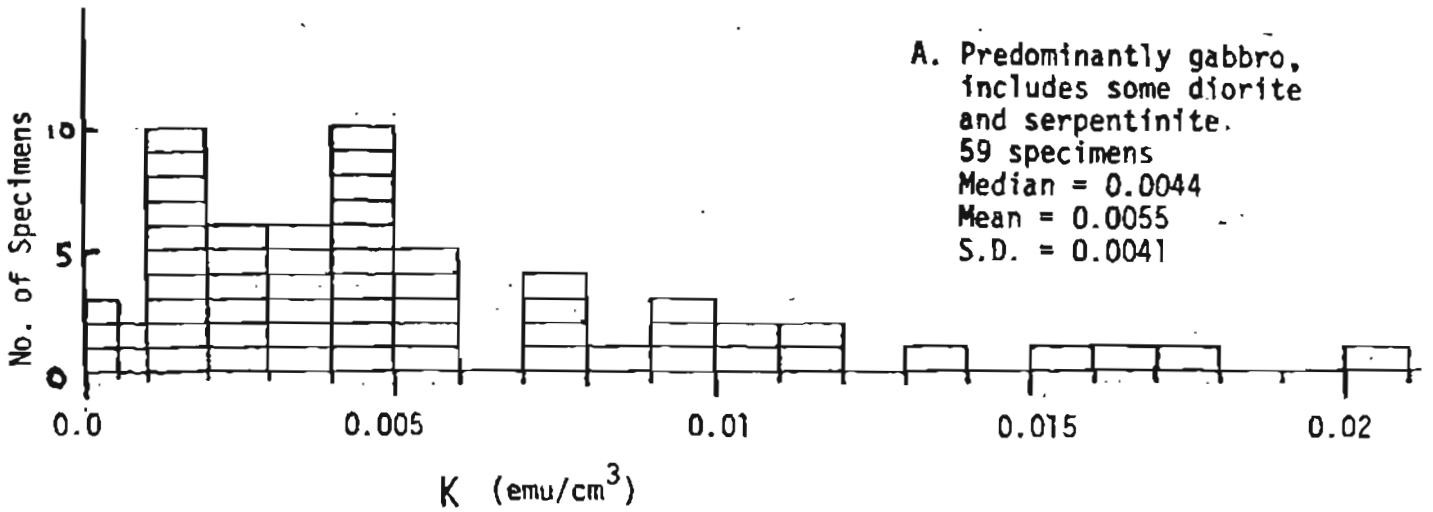

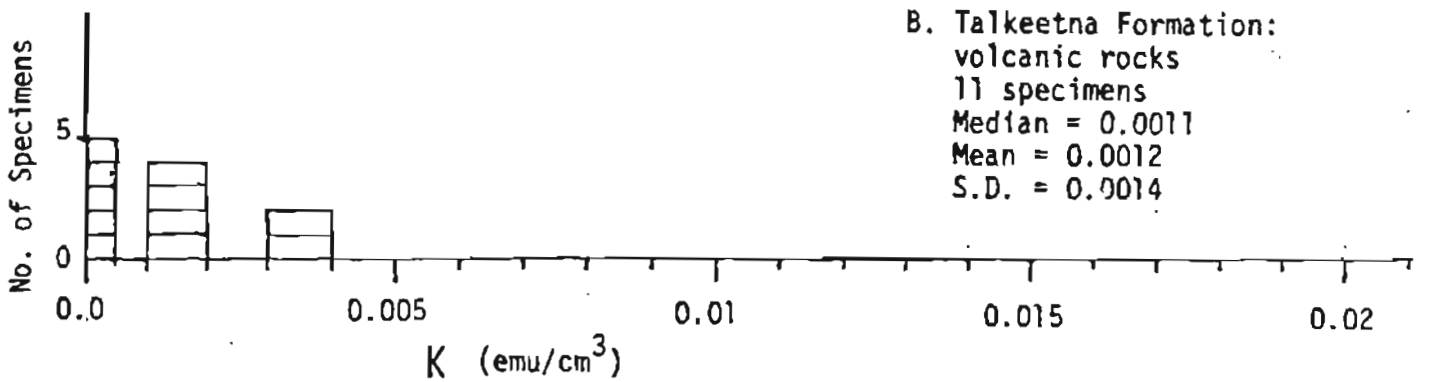

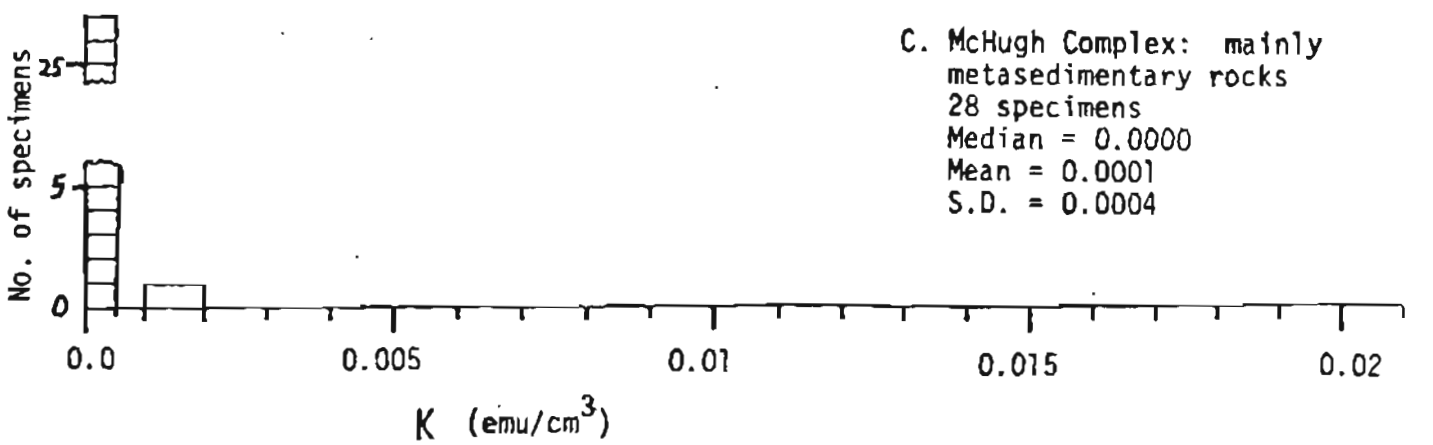

Small regional magnetic fields were removed from the observed profiles. The removed regionals decrease to the south and range approximately from 3 to 12 gammas/ km. The IGRF (1975) for this area is approximately 5 gammas/km in a northeasterly direction.

Computation method:

The magnetic models were computed using a two-dimensional modeling program (twomag, R. Blakely, 1973, USGS).

TABLE 4

Magnetic Properites of Rock Samples (Courtesy of S. Gromme' and J. Hillhouse, U.S.G.S.)

Sample number	Remanent magnetism J X 10 -3	Volume susceptibility K X 10 -3 emu/cubic cm	Permanent magnetism KF X 10 -3	Koenigsberger ratio Q = J/KF	Rock type
ACE125-1	18.3	9.70	5.43	3.36	basalt
ACE125-A	6.5	7.65	4.29	1.52	gabbro
ACE125-B	2.2	11.00	6.16	0.35	gabbro
ACE125-C	0.5	7.66	4.29	0.11	anorthosite
ACE125-D	2.8	11.15	6.25	0.44	gabbro
ACE126-1	0.4	2.56	1.43	0.25	diorite
ACE126-A	2.2	2.82	1.58	1.38	gabbro
ACE126-B	2.9	5.90	3.03	0.86	gabbro
ACE126-C	5.6	1.97	1.10	5.08	diorite
ACE126-D	2.8	1.66	0.93	2.98	gabbro
ACE128-A	0.1	0.91	0.51	0.25	gabbro
ACE133-1	0.4	4.06	2.28	0.18	gabbro
ACE139-H	6.6	4.50	2.52	2.60	serpentine
ACE145-1	1.8	2.82	1.58	1.16	diorite
ACE146-A	5.9	6.00	3.36	1.77	gabbro
ACE146-B	6.9	4.04	2.26	3.06	diabase
ACE147-A	2.7	17.41	9.75	0.28	sheared gab
ACE154-1	0.2	3.45	1.87	0.08	gabbro

Figure 32: Demagnetization curves of two gabbro specimens (Courtesy S. Gromme' and J. Hillhouse, U.S.G.S.)

9A146-B A.F. Demagnetization 6/5/80 JH

#	I	D	J	EXP
1	-53.5	341.0	8.92E-003	0
2	-52.1	342.9	6.38E-003	25
3	-50.8	341.8	4.46E-003	50
4	-49.0	341.9	1.91E-003	100
5	-00.0	341.8	9.97E-004	150
6	-05.5	344.8	8.24E-004	200
7	-06.6	4.8	8.00E-004	300
8	-01.7	43.4	1.04E-003	400
9	-42.2	64.1	1.03E-003	500
10	-29.7	64.9	1.25E-003	600
11	-20.5	00.4	1.20E-003	800
12	-6.8	75.5	1.30E-003	1000

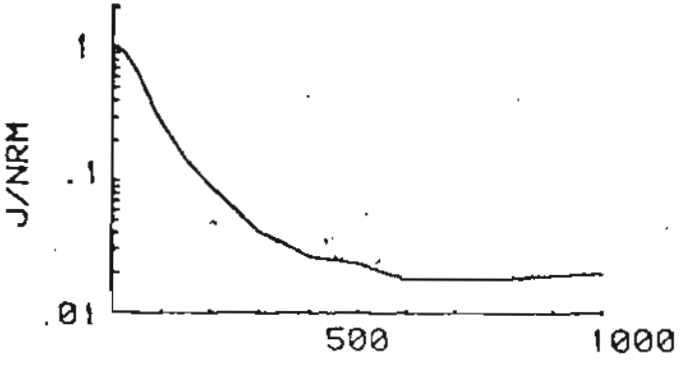

9A125-A A.F. Demagnetization 6/5/80 JH

#	I	D	J	EXP
1	40.4	347.3	8.51E-003	0
2	40.0	359.0	5.56E-003	25
3	40.0	351.1	2.42E-003	50
4	40.4	359.5	8.95E-004	100
5	39.5	359.0	8.44E-004	150
6	15.3	11.0	1.04E-003	200
7	-13.3	17.3	1.40E-003	300
8	-29.0	20.4	1.41E-003	400
9	-02.3	22.3	1.50E-003	500
10	-34.0	14.3	1.40E-003	600
11	-29.0	10.1	1.35E-003	800
12	-40.0	50.0	1.43E-003	1000

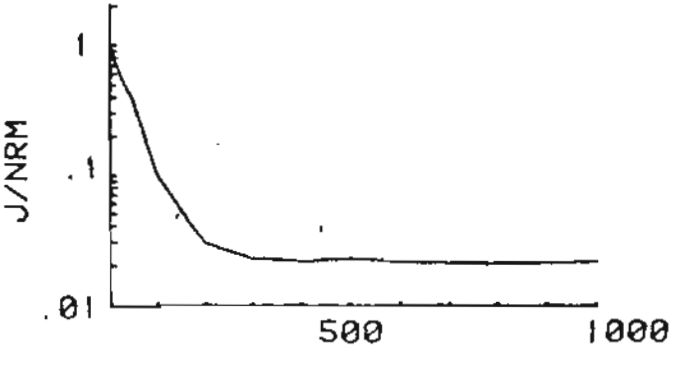

BIBLIOGRAPHY

Andreason, Gordon E., Dempsey, William J., Henderson, John R., and Gilbert, Francis P., 1958, Aeromagnetic map of the Copper River basin, Alaska: U.S. Geological Survey Geophysical Investigation Map GP-156, 1 sheet, scale 1:125,000.

Andreason, Gordon E., Grantz, Arthur, Zietz, Isidore, and Barnes, David F., 1964, Geologic interpretation of magnetic and gravity data in the Copper River basin, Alaska: U. S. Geological Survey Professional Paper 316-H, p. 135-153, 2 sheets, scale 1:250,000.

Barnes, David F., 1977, Bouguer gravity map of the eastern part of southern Alaska: U. S. Geological Survey Open-File Report 77-169-C, 1 sheet, scale 1:1,000,000.

Case, J. E., and MacKevett, E. M., 1976, Aeromagnetic map and geologic interpretation of aeromagnetic map, McCarthy quadrangle, Alaska: U. S. Geological Survey Miscellaneous Field Studies Map MF 773-D, 2 sheets, scale 1:250,000.

Case, J. E., and others, 1979a, Gravity anomaly, Seward and Blying Sound, Alaska: U. S. Geological Survey Miscellaneous Field Studies Map MF 880-C, scale 1:250,000.

Case, J. E., Tysdal, R. G., Hillhouse, J. W., Gromme C. S., 1979b, Geologic interpretation of aeromagnetic map, Seward and Blying Sound quadrangles, Alaska: U. S. Geological Survey Miscellaneous Field Studies Map MF 880-D, 2 sheets, scale 1:250,000.

Clark, Sandra H. B., 1972a, The Wolverine complex, a newly discovered layered ultramafic body in the western Chugach Mountains, Alaska: U. S. Geological Survey Open-File Report 522, 10 p.

Clark, Sandra H. B., 1972b, Reconnaissance bedrock geologic map of the

Chugach Mountains near Anchorage, Alaska: U. S. Geological Survey Miscellaneous Field Studies Map MF-350, 1 sheet, scale 1:250,000.

Clark, Sandra H. B., 1973, The McHugh Complex of South-Central Alaska: U. S. Geological Survey Bulletin 1372-D, p. D1-D11.

Coney, Peter J., Jones, David L., Monger, James W. H., 1980, Cordilleran suspect terranes: Nature, v. 288, p. 329-332.

Connelly, W., 1978, Uyak Complex, Kodiak Islands, Alaska: A Cretaceous subduction complex: Geological Society of America Bulletin, v. 89, no. 12, p. 755-769.

Connelly, William, and Moore, J. Casey., 1979, Geologic map of the northwest side of the Kodiak and adjacent islands, Alaska: U. S. Geological Survey Miscellaneous Field Studies Map MF -1057, 2 sheets, scale 1:250,000.

Detterman, Robert L., and Hartsock, John K., 1966, Geology of the Iniskin-Tuxedni region, Alaska: U. S. Geological Survey Professional Paper 512, 78p, 6 sheets.

Detterman, Robert L., and Reed, Bruce L., 1980, Stratigraphy structure, and economic geology of the Iliamna quadrangle, Alaska: U. S. Geological Survey Bulletin 1368-B, 86p, 1 sheet.

Fischer, Michael A., 1981, Location of the Border Ranges fault southwest of Kodiak Island, Alaska: Geological Society of America Bulletin, Part 1, v. 92, no. 1, p. 19-30.

Grantz, Arthur, 1960, Generalized geologic map of the Nelchina area, Alaska, showing igneous rocks and larger faults: U. S. Geological Survey Miscellaneous Geologic Investigations Map I-312, scale 1:96,000.

Grantz, Arthur, 1961a, Geologic map of the north two-thirds of Anchorage

(D-1) quadrangle, Alaska: U. S. Geological Survey Miscellaneous Geologic Investigations Map I-343, scale 1:48,000.

Grantz, Arthur, 1961b, Geologic map and cross-sections of the Anchorage (D-2) quadrangle and northeasternmost part of the Anchorage (D-3) quadrangle, Alaska: U. S. Geological Survey Miscellaneous Geologic Investigations Map I-342, scale 1:48,000.

Grantz, Arthur, 1965, Geologic map and cross-sections of the Nelchina area, south-central Alaska: U. S. Geological Survey Open-File Report 255, 4 sheets, scale 1:48,000.

Jones, D.L. and Silberling, N. J., 1979, Mesozoic stratigraphy- - the key to tectonic analysis of southern and central Alaska: U. S. Geological Survey Open-File Report 79-1200, 41 p.

MacKevett, E. M., Jr., and Plafker, George, 1974, The Border Ranges fault in south-central Alaska: U. S. Geological Survey Journal of Research, v. 2, no. 3, p. 323-329.

Pavlis, Terry, 1980, Deformation along a Late Mesozoic convergent margin: The Border Ranges fault, southern Alaska: PhD thesis. University of Utah, Salt Lake City, Utah, 84112.

Pessel, G. H., Henning, M. W., and Burns, L. E., 1981, Preliminary geologic map of parts of the Anchorage C-1, C-2, D-1, and D-2 quadrangle, Alaska: Alaska Division of Geologic and Geophysical Surveys Open-File Report AOF-121, 1 sheet, scale 1:63,360.

Plafker, George, and Carnbell, R. B., 1979, The Border Ranges fault in the Saint Elias Mountains, in Johnson, Kathleen M., and Williams, John R., eds., The United States Geological Survey in Alaska; accomplishments during 1978: U. S. Geological Survey Circular 804-B, p. B102-B104.

Plafker, George, Jones, David L., and Pessagno, E. A., Jr., 1977, A Cretaceous accretionary flysch and melange terrane along the Gulf of Alaska margin, in Blean, Kathleen M., ed., The United States Geological Survey in Alaska: accomplishments during 1976: U. S. Geological Survey Circular 751-B, p. B41-B43.

Rose, A. W., 1966, Geology of chromite-bearing ultramafic rocks near Eklutna, Anchorage quadrangle, Alaska: Alaska Division of Mines and Minerals, Geologic Report 18, 20 p.

Tysdal, R. G., and Plafker, George, 1978, Age and continuity of the Valdez Group, southern Alaska, in Sohl, N. F., and Wright, W. B., compilers, Changes in Stratigraphic Nomenclature by the U.S. Geological Survey, 1977: U. S. Geological Survey Bulletin 1457-A, p/ A120-A124.

U. S. Geological Survey, 1979, Aeromagnetic map of part of the Valdez quadrangle, Alaska: U. S. Geological Survey Open-File Map 79-381, 1 sheet, scale 1:250,000.

Winkler, G. R., Silberman, M. L., Grantz, Arthur, Miller, R. J., and MacKevett, E. M., Jr., 1981, Geologic map and summary geochronology of the Valdez quadrangle, southern Alaska: U. S. Geological Survey Open-File Report 80-892A, 2 sheets, scale 1:250,000.